Chapter 5

Gasification Theory and Modeling of Gasifiers

5.1 INTRODUCTION

The design and operation of a gasifier require an understanding of the gasification process and how its design, feedstock, and operating parameters influence the performance of the plant. A good comprehension of the basic reactions is fundamental to the planning, design, operation, troubleshooting, and process improvement of a gasification plant, as is learning the alphabet to read a book. This chapter introduces the basics of the gasification process through a discussion of the reactions involved and the kinetics of the reactions with specific reference to biomass. It also explains how this knowledge can be used to develop a mathematical model of the gasification process.

5.2 GASIFICATION REACTIONS AND STEPS

Gasification is the conversion of solid or liquid feedstock into useful and convenient gaseous fuel or chemical feedstock that can be burned to release energy or used for production of value-added chemicals.

Gasification and combustion are two closely related thermochemical processes, but there is an important difference between them. Gasification packs energy into chemical bonds in the product gas; combustion breaks those bonds to release the energy. The gasification process adds hydrogen to and strips carbon away from the feedstock to produce gases with a higher hydrogen-to-carbon (H/C) ratio, while combustion oxidizes the hydrogen and carbon into water and carbon dioxide, respectively.

A typical biomass gasification process may include the following steps:

- Drying
- Thermal decomposition or pyrolysis
- Partial combustion of some gases, vapors, and char
- Gasification of decomposition products

Pyrolysis is a thermal decomposition process that partially removes carbon from the feed but does not add hydrogen. Gasification, on the other hand,

Biomass Gasification and Pyrolysis. DOI: 10.1016/B978-0-12-374988-8.00005-2

requires a gasifying medium like steam, air, or oxygen to rearrange the molecular structure of the feedstock in order to convert the solid feedstock into gases or liquids; it can also add hydrogen to the product. The use of a medium is essential for the gasification process.

5.2.1 Gasifying Mediums

Gasifying agents react with solid carbon and heavier hydrocarbons to convert them into low-molecular-weight gases like CO and H_2. The main gasifying agents used for gasification are

- Oxygen
- Steam
- Air

Oxygen is a popular gasifying agent, though it is primarily used for the combustion step. It may be supplied to a gasifier either in pure form or through air. The heating value and the composition of the gas produced in a gasifier are strong functions of the nature and amount of the gasifying agent used. A ternary diagram (Figure 5.1) of carbon, hydrogen, and oxygen (see Section 2.4.3) demonstrates the conversion paths of formation of different products in a gasifier.

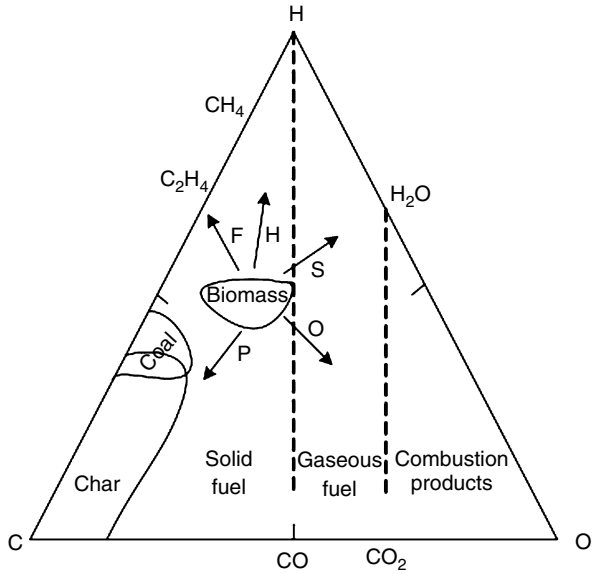

FIGURE 5.1 C-H-O diagram of the gasification process.

TABLE 5.1 Heating Values for Product Gas Based on Gasifying Medium

Medium	Heating Value (MJ/Nm^3)
Air	4–7
Steam	10–18
Oxygen	12–28

If oxygen is used as the gasifying agent, the conversion path moves toward the oxygen corner. Its products include CO for low oxygen and CO_2 for high oxygen. When the amount of oxygen exceeds a certain (stoichiometric) amount, the process moves from gasification to combustion, and the product is "flue gas" instead of "fuel gas." Neither flue gas nor the combustion product contains residual heating value when cooled. A move toward the oxygen corner (Figure 5.1) leads to a lowering of hydrogen content and an increase in carbon-based compounds such as CO and CO_2 in the product gas.

If steam is used as the gasification agent, the path is upward toward the hydrogen corner in Figure 5.1. Then the product gas contains more hydrogen per unit of carbon, resulting in a higher H/C ratio. Some of the intermediate-reaction products like CO and H_2 also help to gasify the solid carbon.

The choice of gasifying agent affects the heating value of the product gas. If air is used instead of oxygen, the nitrogen in it greatly dilutes the product. From Table 5.1, we can see that oxygen gasification has the highest heating value followed by steam and air gasification.

5.3 THE GASIFICATION PROCESS

A typical gasification process generally follows the sequence of steps listed on the next page (illustrated schematically in Figure 5.2).

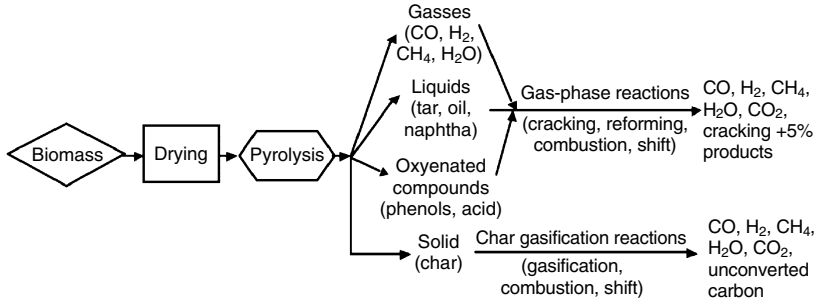

FIGURE 5.2 Potential paths for gasification.

- Preheating and drying
- Pyrolysis
- Char gasification
- Combustion

Though these steps are frequently modeled in series, there is no sharp boundary between them, and they often overlap. The following paragraphs discuss these sequential phases of biomass gasification.

In a typical process, biomass is first heated (dried) and then it undergoes thermal degradation or pyrolysis. The products of pyrolysis (i.e., gas, solid, and liquid) react among themselves as well as with the gasifying medium to form the final gasification product. In most commercial gasifiers, the thermal energy necessary for drying, pyrolysis, and endothermic reactions comes from a certain amount of exothermic combustion reactions allowed in the gasifier. Table 5.2 lists some of the important chemical reactions taking place in a gasifier.

5.3.1 Drying

The typical moisture content of freshly cut wood ranges from 30 to 60%, and for some biomass it can exceed 90% (see Table 2.9). Every kilogram of moisture in the biomass takes away a minimum of 2260 kJ of extra energy from the gasifier to vaporize water, and that energy is not recoverable. For a high level of moisture this loss is a concern, especially for energy applications. While we cannot do much about the inherent moisture residing within the cell structure, efforts may be made to drive away the external or surface moisture. A certain amount of predrying is thus necessary to remove as much moisture from the biomass as possible before it is fed into the gasifier. For the production of a fuel gas with a reasonably high heating value, most gasification systems use dry biomass with a moisture content of 10 to 20%.

The final drying takes place after the feed enters the gasifier, where it receives heat from the hot zone downstream. This heat dries the feed, which releases water. Above 100 °C, the loosely bound water that is in the biomass is irreversibly removed. As the temperature rises, the low-molecular-weight extractives start volatilizing. This process continues until a temperature of approximately 200 °C is reached.

5.3.2 Pyrolysis

In pyrolysis no external agent is added. In a slow pyrolysis process, the solid product moves toward the carbon corner of the ternary diagram, and more char is formed. In fast pyrolysis, the process moves toward the C-H axis opposite the oxygen corner (Figure 5.1). The oxygen is largely diminished, and thus we expect more liquid hydrocarbon.

TABLE 5.2 Typical Gasification Reactions at 25 °C

Reaction Type	Reaction
Carbon Reactions	
R1 (Boudouard)	$C + CO_2 \leftrightarrow 2CO + 172$ kJ/mol[1]
R2 (water-gas or steam)	$C + H_2O \leftrightarrow CO + H_2 + 131$ kJ/mol[2]
R3 (hydrogasification)	$C + 2H_2 \leftrightarrow CH_4 - 74.8$ kJ/mol[2]
R4	$C + 0.5\ O_2 \rightarrow CO - 111$ kJ/mol[1]
Oxidation Reactions	
R5	$C + O_2 \rightarrow CO_2 - 394$ kJ/mol[2]
R6	$CO + 0.5O_2 \rightarrow CO_2 - 284$ kJ/mol[4]
R7	$CH_4 + 2O_2 \leftrightarrow CO_2 + 2H_2O - 803$ kJ/mol[3]
R8	$H_2 + 0.5\ O_2 \rightarrow H_2O - 242$ kJ/mol[4]
Shift Reaction	
R9	$CO + H_2O \leftrightarrow CO_2 + H_2 - 41.2$ kJ/mol[4]
Methanation Reactions	
R10	$2CO + 2H_2 \rightarrow CH_4 + CO_2 - 247$ kJ/mol[4]
R11	$CO + 3H_2 \leftrightarrow CH_4 + H_2O - 206$ kJ/mol[4]
R14	$CO_2 + 4H_2 \rightarrow CH_4 + 2H_2O - 165$ kJ/mol[2]
Steam-Reforming Reactions	
R12	$CH_4 + H_2O \leftrightarrow CO + 3H_2 + 206$ kJ/mol[3]
R13	$CH_4 + 0.5\ O_2 \rightarrow CO + 2H_2 - 36$ kJ/mol[3]

[1]*Source:* Higman and van der Burgt, 2008, p. 12.
[2]*Source:* Klass, 1998, p. 276.
[3]*Source:* Higman and van der Burgt, 2008, p. 3.
[4]*Source:* Knoef, 2005, p. 15.

Pyrolysis, which precedes gasification, involves the thermal breakdown of larger hydrocarbon molecules of biomass into smaller gas molecules (condensable and noncondensable) with no major chemical reaction with air, gas, or any other gasifying medium. For a detailed description of this process, see Chapter 3.

One important product of pyrolysis is tar formed through condensation of the condensable vapor produced in the process. Being a sticky liquid, tar creates a great deal of difficulty in industrial use of the gasification product. A discussion of tar formation and ways of cracking or reforming it into useful noncondensable gases is presented in Chapter 4.

5.3.3 Char Gasification Reactions

The gasification step that follows pyrolysis involves chemical reactions among the hydrocarbons in fuel, steam, carbon dioxide, oxygen, and hydrogen in the reactor, as well as chemical reactions among the evolved gases. Of these, char gasification is the most important. The char produced through pyrolysis of biomass is not necessarily pure carbon. It contains a certain amount of hydrocarbon comprising hydrogen and oxygen.

Biomass char is generally more porous and reactive than coke. Its porosity is in the range of 40 to 50% while that of coal char is 2 to 18%. The pores of biomass char are much larger (20–30 micron) than those of coal char (~5 angstrom) (Encinar et al., 2001). Thus, its reaction behavior is different from that of chars derived from coal, lignite, or peat. For example, the reactivity of peat char decreases with conversion or time, while the reactivity of biomass char increases with conversion (Figure 5.3). This reverse trend can be attributed to the increasing catalytic activity of the biomass char's alkali metal constituents (Risnes et al., 2001).

Gasification of biomass char involves several reactions between the char and the gasifying mediums. Following is a description of some of those reactions with carbon, carbon dioxide, hydrogen, steam, and methane.

$$\text{Char} + O_2 \rightarrow CO_2 \text{ and } CO \tag{5.1}$$

$$\text{Char} + CO_2 \rightarrow CO \tag{5.2}$$

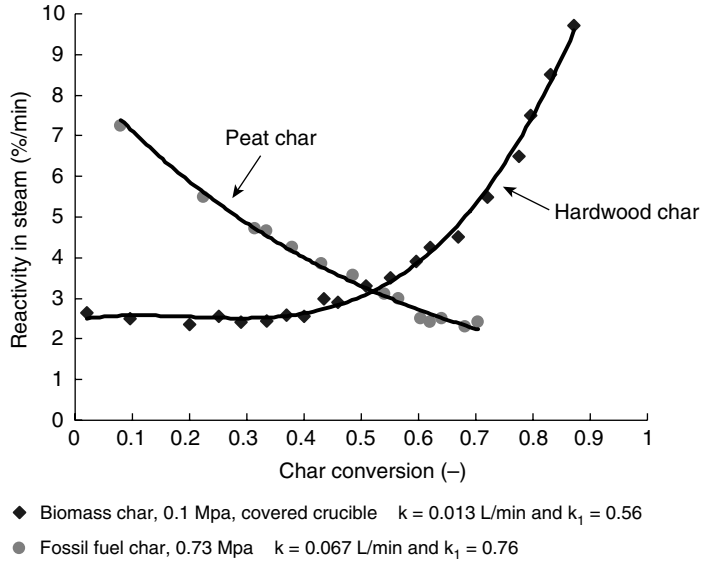

FIGURE 5.3 Reactivities of peat char for gasification in steam decrease with conversion; reactivities of hardwood char increase with conversion. *(Source: Data from Liliedahl and Sjostrom, 1997.)*

$$\text{Char} + H_2O \rightarrow CH_4 \text{ and } CO \tag{5.3}$$

$$\text{Char} + H_2 \rightarrow CH_4 \tag{5.4}$$

Equations (5.1) through (5.4) show how gasifying agents like oxygen, carbon dioxide, and steam react with solid carbon to convert it into lower-molecular-weight gases like carbon monoxide and hydrogen. Some of the reactions are known by the names listed in Table 5.2.

Gasification reactions are generally endothermic, but some of them can be exothermic as well. For example, those of carbon with oxygen and hydrogen (R3, R4, and R5 in Table 5.2) are exothermic, whereas those with carbon dioxide and steam (reactions R1 and R2) are endothermic. The heat of reaction given in Table 5.2 for various reactions refers to a temperature of 25 °C.

Speed of Char Reactions

The rate of gasification of char (comprising of mainly carbon) depends primarily on its reactivity and the reaction potential of the gasifying medium. Oxygen, for example, is the most active, followed by steam and carbon dioxide. The rate of the char–oxygen reaction ($C + 0.5O_2 \rightarrow CO$) is the fastest among the four in Table 5.2 (R1, R2, R3, and R4). It is so fast that it quickly consumes the oxygen, leaving hardly any free oxygen for any other reactions.

The rate of the char–steam reaction ($C + H_2O \rightarrow CO + H_2$) is three to five orders of magnitude slower than that of the char–oxygen reaction. The Boudouard, or char–carbon dioxide, reaction ($C + CO_2 \rightarrow 2CO$) is six to seven orders of magnitude slower (Smoot and Smith, 1985). The rate of the water–gas or water–steam gasification reaction (R2) is about two to five times faster than that of the Boudouard reaction (R1) (Blasi, 2009).

The char–hydrogen reaction that forms methane ($C + 2H_2 \rightarrow CH_4$) is the slowest of all. Walker et al. (1959) estimated the relative rates of the four reactions, at 800 °C temperature and 10 K Pa pressure, as 10^5 for oxygen, 10^3 for steam, 10^1 for carbon dioxide, and 3×10^{-3} for hydrogen. The relative rates, R, may be shown as

$$R_{C+O_2} >> R_{C+H_2O} > R_{C+CO_2} >> R_{C+H_2} \tag{5.5}$$

When steam reacts with carbon it can produce CO and H_2. Under certain conditions the steam and carbon reaction can also produce CH_4 and CO_2.

Boudouard Reaction Model

The gasification of char in carbon dioxide is popularly known as the *Boudouard reaction*.

$$C + CO_2 \leftrightarrow 2CO \text{ (reaction R1 in Table 5.2)} \tag{5.6}$$

Blasi (2009) describes the Boudouard reaction through the following steps. In the first step, CO_2 dissociates at a carbon-free active site (C_{fas}), releasing carbon

monoxide and forming a carbon–oxygen surface complex, C(O). This reaction can move in the opposite direction as well, forming a carbon active site and CO_2 in the second step. In the third step, the carbon–oxygen complex produces a molecule of CO.

$$\text{Step 1} \quad C_{fas} + CO_2 \xrightarrow{k_{b1}} C(O) + CO \tag{5.7}$$

$$\text{Step 2} \quad C(O) + CO \xrightarrow{k_{b2}} C_{fas} + CO_2 \tag{5.8}$$

$$\text{Step 3} \quad C(O) \xrightarrow{k_{b3}} CO \tag{5.9}$$

where k_i is the rate of the ith reaction.

The rate of the char gasification reaction in CO_2 is insignificant: below 1000 K.

Water–Gas Reaction Model

The gasification of char in steam, known as the *water–gas reaction*, is perhaps the most important gasification reaction.

$$C + H_2O \leftrightarrow CO + H_2 \,(\text{R2 in Table 5.2}) \tag{5.10}$$

The first step involves the dissociation of H_2O on a free active site of carbon (C_{fas}), releasing hydrogen and forming a surface oxide complex of carbon C(O). In the second and third steps, the surface oxide complex produces a new free active site and a molecule of CO.

$$\text{Step 1} \quad C_{fas} + H_2O \xrightarrow{k_{w1}} C(O) + H_2 \tag{5.11}$$

$$\text{Step 2} \quad C(O) + H_2 \xrightarrow{k_{w2}} C_{fas} + H_2O \tag{5.12}$$

$$\text{Step 3} \quad C(O) \xrightarrow{k_{w3}} CO \tag{5.13}$$

Some models (Blasi, 2009) also include the possibility of hydrogen inhibition by C(H) or $C(H)_2$ complexes as here:

$$C_{fas} + H_2 \leftrightarrow C(H)_2 \tag{5.14}$$

$$C_{fas} + 0.5\,H_2 \leftrightarrow C(H) \tag{5.15}$$

The presence of hydrogen has a strong inhibiting effect on the char gasification rate in H_2O. For example, 30% hydrogen in the gasification atmosphere can reduce the gasification rate by a factor as high as 15 (Barrio et al., 2001). So an effective means of accelerating the water–gas reaction is continuous removal of hydrogen from the reaction site.

Shift Reaction Model

The shift reaction is an important gas-phase reaction. It increases the hydrogen content of the gasification product at the expense of carbon monoxide. This reaction is also called the "water–gas shift reaction" in some literature (Klass, 1998, p. 277), though it is much different from the water–gas reaction (R2).

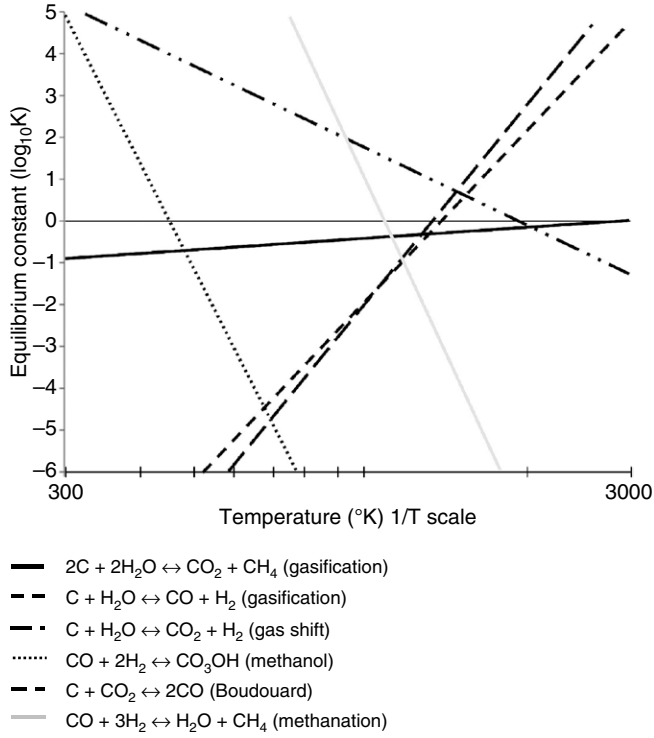

FIGURE 5.4 Equilibrium constants for selected gasification reactions. *(Source: Adapted from Probstein and Hicks, 2006, p. 63.)*

$$CO + H_2O \leftrightarrow CO_2 + H_2 - 41.2 \text{ kJ/mol (reaction R9 in Table 5.2)} \quad (5.16)$$

This is a prestep in syngas production in the downstream of a gasifier, where the ratio of hydrogen and carbon monoxide in the product gas is critical.

The shift reaction is slightly exothermic, and its equilibrium yield decreases slowly with temperature. Depending on temperature, it may be driven in either direction—that is, products or reactants. However, it is not sensitive to pressure (Petersen and Werther, 2005).

Above 1000 °C the shift reaction (R9) rapidly reaches equilibrium, but at a lower temperature it needs heterogeneous catalysts. Figure 5.4 (Probstein and Hicks, 2006, p. 63) shows that this reaction has a higher equilibrium constant at a lower temperature, which implies a higher yield of H_2 at a lower temperature. With increasing temperature, the yield decreases but the reaction rate increases. Optimum yield is obtained at about 225 °C.

Because the reaction rate at such a low temperature is low, catalysts like chromium-promoted iron, copper-zinc, and cobalt-molybdenum are used (Probstein and Hicks, 2006, p. 124). At higher temperatures (350–600 °C) Fe-based

catalysts may be employed. Pressure exerts no appreciable effect on the H_2/CO ratio. Commercial shift conversions of CO use these catalysts (Boerrigter and Rauch, 2005):

- Copper-promoted catalyst, at about 300–510 °C
- Copper-zinc-aluminum oxide catalyst, at about 180–270 °C

Hydrogasification Reaction Model

This reaction involves the gasification of char in a hydrogen environment, which leads to the production of methane.

$$C + 2H_2 \rightarrow CH_4 \text{ (reaction R3 in Table 5.2)} \tag{5.17}$$

The rate of this reaction is much slower than that of the other reactions, and so it is not discussed here. It is of importance only when the production of synthetic natural gas (SNG) is desired.

5.3.4 Char Combustion Reactions

Most gasification reactions are endothermic. To provide the required heat of reaction as well as that required for heating, drying, and pyrolysis, a certain amount of exothermic combustion reaction is allowed in a gasifier. Reaction R5 ($C + O_2 \rightarrow CO_2$) is the best in this regard as it gives the highest amount of heat (394 kJ) per k.mol of carbon consumed. The next best is R4 ($C + 1/2O_2 \rightarrow CO$), which also produces the fuel gas CO, but produces only 111 kJ/mol of heat. The speed of R4 is relatively slow.

When carbon comes in contact with oxygen, both R4 and R5 can take place, but their extent depends on temperature. A partition coefficient, β, may be defined to determine how oxygen will partition itself between the two. R4 and R5 may be combined and written as

$$\beta C + O_2 \rightarrow 2(\beta - 1)CO + (2 - \beta)CO_2 \tag{5.18}$$

The value of the partition coefficient β lies between 1 and 2 and depends on temperature. One of the commonly used expressions (Arthur, 1951) for β is

$$\beta = \frac{[CO]}{[CO_2]} = 2400e^{-\left(\frac{6234}{T}\right)} \tag{5.19}$$

where T is the surface temperature of the char.

Combustion reactions are generally faster than gasification reactions under similar conditions. Table 5.3 compares the rate of combustion and gasification for a biomass char at a typical gasifier temperature of 900 °C. The combustion rates are at least one order of magnitude faster than the gasification reaction rate. Owing to pore diffusion resistance, finer char particles have a much higher reaction rate.

TABLE 5.3 Comparison of the Effect of Pore Diffusion on Char Gasification and Combustion Rates

Particle Size (μm)	Combustion Rate (min^{-1})	Gasification Rate (min^{-1})	Combustion Rate/ Gasification Rate (–)
6350	0.648	0.042	15.4
841	5.04	0.317	15.9
74	55.9	0.975	57.3

Source: Adapted from Reed, 2002, p. II-189.

Another important difference between char gasification and combustion reactions in a fluidized bed is that during gasification the temperature of the char particle is nearly the same as the bed temperature because of simultaneous exothermic and endothermic reactions on it (Gomez-Barea et al., 2008). In combustion, the char particle temperature can be much hotter than the bed temperature (Basu, 1977).

The relative amounts of fuel, oxidant (air or oxygen), and steam (if used) govern the fraction of carbon or oxygen that enters R5 or R4 (Table 5.2). Any more oxidant than that needed for the endothermic reaction will increase the gasifier temperature unnecessarily as well as reduce the quality of the product by diluting it with carbon dioxide. Example 5.1 illustrates how the heat balance works out in a gasifier.

Example 5.1

In an updraft gasifier, the water–gas gasification reaction ($C + H_2O \rightarrow CO + H_2$ + 131 kJ/mol) is to be carried out. Assume that drying and other losses in the system need 50% additional heat. Find a means to adjust the extent of the combustion reaction by controlling the supply of oxygen and carbon such that this need is met.

Solution

The reaction needs 131 kJ of heat for gasification of each mol of carbon. In oxygen-deficient or substoichiometric conditions like that present in a gasifier, the exothermic combustion reaction ($C + 1/2O_2 \rightarrow CO$ − 111 kJ/mol) is more likely to take place than the more complete combustion reaction ($C + O_2 \rightarrow CO_2$ − 394 kJ/mol). If we adjust the feedstock such that for every mole of carbon gasified, only p moles of carbon will be partially oxidized using $p/2$ mol of oxygen, the heat released by the combustion reaction will exactly balance the heat needed by the gasification reaction. In that case the reaction is

$$C + H_2O \rightarrow CO + H_2 + 131\,kJ/mol \quad \text{(i)}$$

- Heat required for endothermic reaction/k.mol C = 131 kJ
- Heat required for drying, etc. = 0.5 × 131 = 65.5 kJ
- Total heat required = 131 + 65.5 = 196.5 kJ

If p moles of carbon participate in the exothermic reaction, R4,

$$pC + 0.5pO_2 \rightarrow pCO - 111p \qquad \text{(ii)}$$

Then we have $111p = 196.5$ or $p = 1.77$

Adding reactions (i) and (ii), we get the net reaction

$$2.77C + H_2O + 0.88O_2 \rightarrow 1.77CO + H_2$$

Thus, for (2.77 × 12) kg of carbon, we need (2 + 16) kg of steam and (0.88 × 32) kg of oxygen. If we add more oxygen, the combustion reaction, R5, may take place and the temperature of the combustion zone may rise further.

5.3.5 Catalytic Gasification

Use of catalysts in the thermochemical conversion of biomass may not be essential, but it can help under certain circumstances. Two main motivations for catalysts are:

- Removal of tar from the product gas, especially if the downstream application or the installed equipment cannot tolerate it (see Chapter 4 for more details).
- Reduction in methane content of the product gas, particularly when it is to be used as syngas (CO, H_2 mixture).

The development of catalytic gasification is driven by the need for tar reforming. When the product gas passes over the catalyst particles, the tar or condensable hydrocarbon can be reformed on the catalyst surface with either steam or carbon dioxide, thus producing additional hydrogen and carbon monoxide. The reactions may be written in simple form as

Steam reforming reaction:

$$C_nH_m + nH_2O \xrightarrow{\text{catalyst}} (n + m/2)H_2 + nCO \qquad (5.20)$$

Carbon dioxide (or dry) reforming reaction:

$$C_nH_m + nCO_2 \xrightarrow{\text{catalyst}} 2nCO + (m/2)H_2 \qquad (5.21)$$

As we can see, instead of undesirable tar or soot, we get additional fuel gases through the catalytic tar-reforming reactions (Eq. 5.20). Both gas yield and the heating value of the product gas improve.

The other option for tar removal is thermal cracking, but it requires a high (>1100 °C) temperature and produces soot; thus, it cannot harness the lost energy in tar hydrocarbon.

The second motivation for catalytic gasification is removal of methane from the product gas. For this we can use either catalytic steam reforming or catalytic

carbon dioxide reforming of methane. Reforming is very important for the production of syngas, which cannot tolerate methane and requires a precise ratio of CO and H_2 in the product gas. In steam reforming, methane reacts with steam in the temperature range of 700 to 1100 °C in the presence of a metal-based catalyst, and thus it is reformed into CO and H_2 (Li et al., 2007):

$$CH_4 + H_2O \xrightarrow{\text{catalyst}} CO + 3H_2 + 206\ \text{kJ/mol} \quad \text{– steam reforming of methane} \tag{5.22}$$

This reaction is widely used in hydrogen production from methane, for which nickel-based catalysts are very effective.

The carbon dioxide reforming of methane is not as widely used commercially as steam reforming, but it has the special attraction of reducing two greenhouse gases (CO_2 and CH_4) in one reaction, and it can be a good option for removal of carbon dioxide from the product gas. The reaction is highly endothermic (Wang and Lu, 1996):

$$CH_4 + CO_2 \xrightarrow{\text{catalyst}} 2CO + 2H_2 + 247\ \text{kJ/mol} \quad \text{– dry reforming of methane} \tag{5.23}$$

Nickel-based catalysts are also effective for the dry-reforming reaction (Liu et al., 2008).

Catalyst Selection

Catalysts for reforming reactions are to be chosen keeping in view their objective and practical use. Some important catalyst selection criteria for the removal of tar are as follows:

- Effective
- Resistant to deactivation by carbon fouling and sintering
- Easily regenerated
- Strong and resistant to attrition
- Inexpensive

For methane removal, the following criteria are to be met in addition to those in the previous list:

- Capable of reforming methane
- Must provide the required CO/H_2 ratio for the syngas process

Catalysts can work in in-situ and post-gasification reactions. The former may involve impregnating the catalyst in the biomass prior to gasification. It can be added directly in the reactor, as in a fluidized bed. Such application is effective in reducing the tar, but it is not effective in reducing methane (Sutton et al., 2001). In post-gasification, catalysts are placed in a secondary reactor downstream of the gasifier to convert the tar and methane formed. This has the additional advantage of being independent of the gasifier operating condition.

The second reactor can be operated at temperatures optimum for the reforming reaction.

The catalysts in biomass gasification are divided into three groups: earth metal, alkali metal, and nickel based.

Earth metal catalysts. Dolomite ($CaCO_3.MgCO_3$) is very effective for disposal of tar, and it is inexpensive and widely available, obviating the need for catalyst regeneration. It can be used as a primary catalyst by mixing with the biomass or as a secondary catalyst in a reformer downstream, which is also called a *guard bed*. Calcined dolomite is significantly more effective than raw dolomite (Sutton et al., 2001). Neither, however, is very useful for methane conversion. The rate of the reforming reaction is higher with carbon dioxide than with steam.

Alkali metal catalysts. Potassium carbonate and sodium carbonate are important in biomass gasification as primary catalysts. K_2CO_3 is more effective than Na_2CO_3. Unlike dolomite, they can reduce methane in the product gas through a reforming reaction. Many biomass types have inherent potassium in their ash, so they can benefit from the catalytic action of the potassium with reduced tar production. However, potassium is notorious for agglomerating in fluidized beds, which offsets its catalytic benefit.

Ni-based catalyst. Nickel is highly effective as a reforming catalyst for reduction of tar as well as for adjustment of the CO/H_2 ratio through methane conversion. It performs best when used downstream of the gasifier in a secondary bed, typically at 780 °C (Sutton et al., 2001). Deactivation of the catalyst with carbon deposits is an issue. Nickel is relatively inexpensive and commercially available though not as cheap as dolomite. Appropriate catalyst support is important for optimum performance.

5.3.6 Gasification Processes in the Reactors

The sequence of gasification reactions depends to some extent on the type of gas–solid contacting reactors used. A brief description of this process as it occurs in some principal reactor types follows.

Moving-Bed Reactor

To explain the reaction process in moving-bed gasifiers, we take the example of a simple updraft gasifier reactor (Figure 5.5).

In a typical updraft gasifier, fuel is fed from the top; the product gas leaves from the top as well. The gasifying agent (air, oxygen, steam, or their mixture), is slightly preheated and enters the gasifier through a grid at the bottom. The gas then rises through a bed of descending fuel or ash in the gasifier chamber.

The air (the gasifying medium), as it enters the bottom of the bed, meets hot ash and unconverted chars descending from the top (Figure 5.5). The

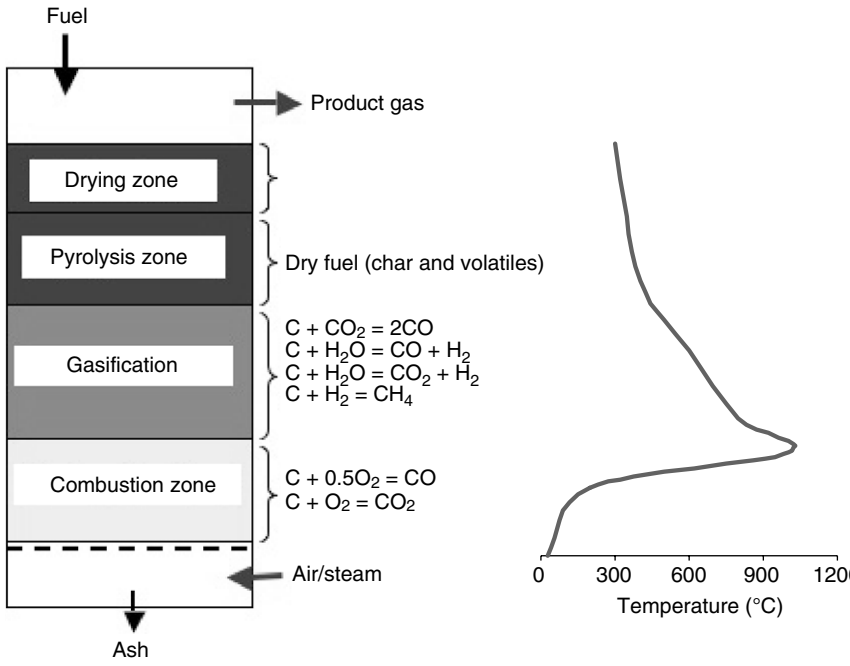

FIGURE 5.5 Stages of gasification in an updraft gasifier.

temperature in the bottom layer well exceeds the ignition temperature of carbon, so the highly exothermic combustion reaction (Eq. 5.24) takes place in the presence of excess oxygen. The released heat heats the upward-moving gas as well as the descending solids.

$$C + O_2 \rightarrow CO_2 - 394\ \text{kJ/mol} \tag{5.24}$$

The combustion reaction (Eq. 5.24), being very fast, rapidly consumes most of the available oxygen. As the available oxygen is reduced further up, the combustion reaction changes into partial combustion, releasing CO and a moderate amount of heat.

$$C + 1/2\,O_2 \rightarrow CO - 111\ \text{kJ/mol} \tag{5.25}$$

The hot gas, a mixture of CO, CO_2, and steam (from the feed and the gasifying medium), moves further up into the gasification zone, where char from the upper bed is gasified by Eq. (5.26). The carbon dioxide concentration increases rapidly in the first combustion zone, but once the oxygen is nearly depleted, the CO_2 enters the gasification reaction (Eq. 5.26) with char, resulting in a decline in CO_2 concentration in the gasification zone.

$$C + CO_2 \rightarrow 2CO + 172\ \text{kJ/mol} \tag{5.26}$$

$$C + H_2O \rightarrow CO + H_2 + 131\ \text{kJ/mol}$$

Sensible heating of the hot gas provides the heat for the two endothermic gasification reactions in Eq. (5.26): R1 and R2 (Table 5.2). These are responsible for most of the gasification products like hydrogen and carbon monoxide. Because of their endothermic nature, the temperature of the gas reduces.

The zone above the gasification zone is for the pyrolysis of biomass. The residual heat of the rising hot gas heats up the dry biomass, descending from above. The biomass then decomposes (pyrolyzed) into noncondensable gases, condensable gases, and char. Both gases move up while the solid char descends with other solids.

The topmost zone dries the fresh biomass fed into it using the balance enthalpy of the hot product gas coming from the bottom. This gas is a mixture of gasification and pyrolysis products.

In an updraft gasifier biomass fed from the top descends, while air injected from the side meets with the pyrolysis product, releasing heat (see Chapter 6). Thereafter, both product gas and solids (char and ash) move down in the downdraft gasifier. Here, a part of the pyrolysis gas may burn above the gasification zone. Thus, the thermal energy required for drying, pyrolysis, and gasification is supplied by the combustion of pyrolysis gas. This phenomenon is called *flaming pyrolysis*.

In downdraft gasifiers, the reaction regions are different from those for updraft gasifiers. Here, steam and oxygen or air are fed into a lower section of the gasifier (Figure 5.6) with the biomass. The pyrolysis and combustion products flow downward. The hot gas then moves downward over the remaining

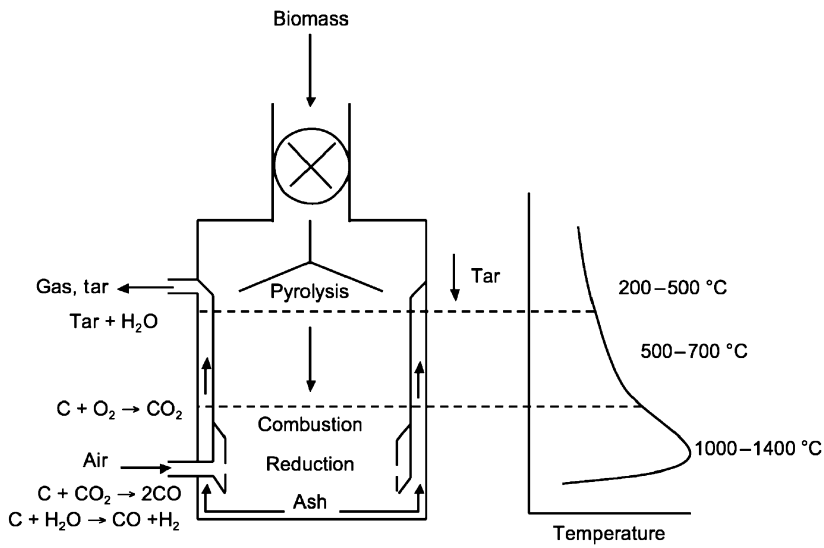

FIGURE 5.6 Gasification reactions in a downdraft gasifier.

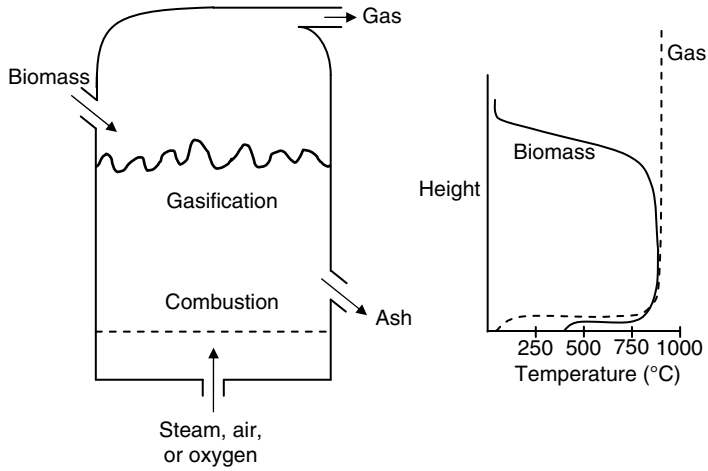

FIGURE 5.7 Schematic of a bubbling fluidized-bed gasifier. *(Source: Higman and van der Burgt, 2008, p. 106.)*

hot char, where gasification takes place. Such an arrangement results in tar-free but low-energy-content gases.

Fluidized-Bed Reactor

In a bubbling fluidized bed, the fuel fed from either the top or the sides mixes relatively fast over the whole body of the fluid bed (Figure 5.7). The gasifying medium (air, oxygen, steam, or their mixture) also serves as the fluidizing gas and so is sent through the bottom of the reactor.

In a typical fluidized-bed gasifier, fresh solid fuel particles are brought into contact with hot bed solids that quickly heat the particles to the bed temperature and make them undergo rapid drying and pyrolysis, producing char and gases.

Though the bed solids are well mixed, the fluidizing gas remains generally in plug-flow mode, entering from the bottom and leaving from the top. Upon entering the bottom of the bed, the oxygen goes into fast exothermic reactions (R4, R5, and R8 in Table 5.2) with char mixed with bed materials. The bed materials immediately disperse the heat released by these reactions to the entire fluidized bed. The amount of heat released near the bottom grid depends on the oxygen content of the fluidizing gas and the amount of char that comes in contact with it. The local temperature in this region depends on how vigorously the bed solids disperse heat from the combustion zone.

Subsequent gasification reactions take place further up as the gas rises. The bubbles of the fluidized bed can serve as the primary conduit to the top. They are relatively solids-free. While they help in mixing, the bubbles can also allow gas to bypass the solids without participating in the gasification reactions. The pyrolysis products coming in contact with the hot solids break down into

noncondensable gases. If they escape the bed and rise into the cooler freeboard, tar and char are formed.

A bubbling fluidized bed cannot achieve complete char conversion because of the back-mixing of solids. The high degree of solid mixing helps a bubbling fluidized-bed gasifier achieve temperature uniformity, but owing to the intimate mixing of fully gasified and partially gasified fuel particles, any solids leaving the bed contain some partially gasified char. Char particles entrained from a bubbling bed can also contribute to the loss in a gasifier. The other important problem with fluidized-bed gasifiers is the slow diffusion of oxygen from the bubbles to the emulsion phase. This encourages the combustion reaction in the bubble phase, which decreases gasification efficiency.

In a circulating fluidized bed (CFB), solids circulate around a loop that is characterized by intense mixing and longer solid residence time within its solid circulation loop. The absence of any bubbles avoids the gas-bypassing problem of bubbling fluidized beds.

Fluidized-bed gasifiers typically operate in the temperature range of 800 to 1000 °C to avoid ash agglomeration. This is satisfactory for reactive fuels such as biomass, municipal solid waste (MSW), and lignite. Since fluidized-bed gasifiers operate at relatively low temperatures, most high-ash fuels, depending on ash chemistry, can be gasified without the problem of ash sintering and agglomeration. Owing to the large thermal inertia and vigorous mixing in fluidized-bed gasifiers, a wider range of fuels or a mixture of them can be gasified. This feature is especially attractive for biomass fuels, such as agricultural residues and wood, that may be available for gasification at different times of the year. For these reasons, many developmental activities on large-scale biomass gasification are focused on fluidized-bed technologies.

Entrained-Flow Reactor

Entrained-flow gasifiers are preferred for the integrated gasification combined cycle (IGCC) plants. Reactors of this type typically operate at 1400 °C and 20 to 70 bar pressure, where powdered fuel is entrained in the gasifying medium. Figure 5.8 shows two entrained-flow gasifier types. In the first one, oxygen, the most common gasifying medium, and the powdered fuel enter from the side; in the second one they enter from the top.

In entrained-flow gasifiers, the combustion reaction, R5 (Eq. 5.24), may take place right at the entry point of the oxygen, followed by reaction R4 (Eq. 5.25) further downstream, where the excess oxygen is used up.

Powdered fuel (< 75 micron) is injected into the reactor chamber along with oxygen and steam (air is rarely used). To facilitate feeding into the reactor, especially if it is pressurized, the fuel may be mixed with water to make a slurry. The gas velocity in the reactor is sufficiently high to fully entrain the fuel particles. Slurry-fed gasifiers need additional reactor volume for evaporation of the large amount of water mixed with the fuel. Furthermore, their oxygen

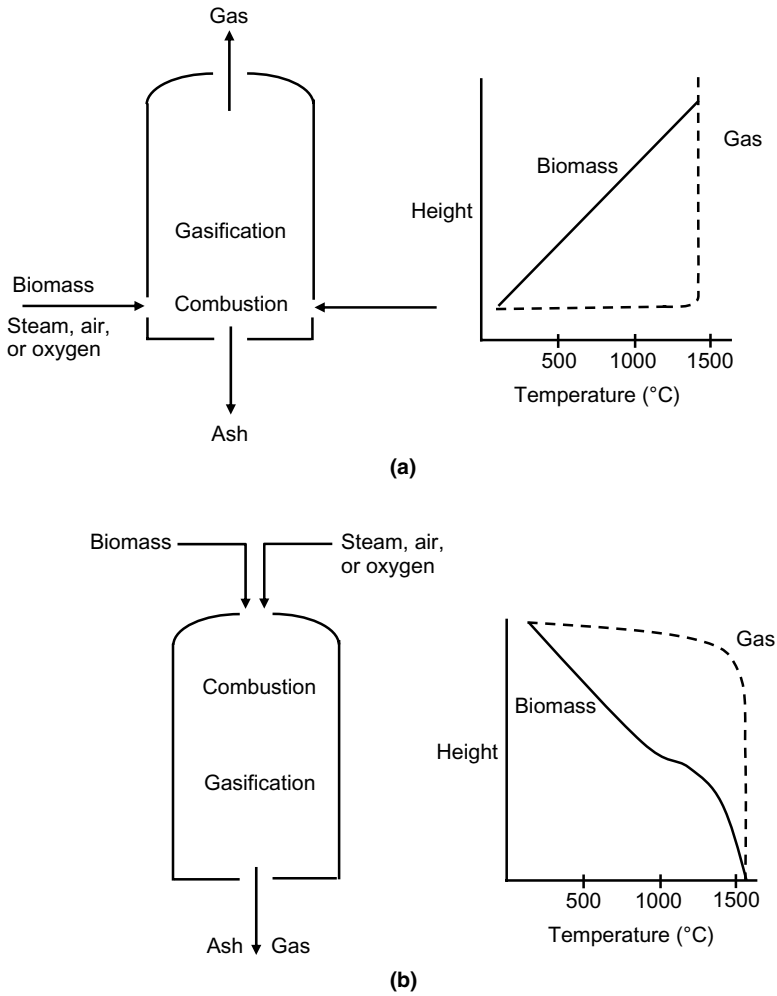

FIGURE 5.8 Two main types of entrained-flow gasifiers: (a) side-fed entrained-flow reactor, and (b) top-fed entrained-flow reactor.

consumption is about 20% greater than that of a dry-feed system owing to higher blast requirements (Higman and van der Burgt, 2008).

Entrained flow gasifiers are of two types depending on how and where the fuel is injected into the reactor. Chapter 6 discusses several types. In all of these designs, oxygen, upon entering the reactor, reacts rapidly with the volatiles and char in exothermic reactions. These raise the reactor temperature well above the melting point of ash, resulting in complete destruction of tar or oil. Such high temperatures should give a very high level of carbon conversion.

An entrained-flow gasifier may be viewed as a plug-flow reactor. Although the gas is heated to the reactor temperature rapidly upon entering, solids heat up less slowly along the reactor length because of the reactor's large thermal capacity and plug-flow nature, as shown in Figure 5.8. Some entrained-flow reactors are modeled as stirred tank reactors because of the rapid mixing of solids.

5.4 KINETICS OF GASIFICATION

Stoichiometric calculations can help determine the products of reaction. Not all reactions are instantaneous and completely convert reactants into products. Many of the chemical reactions discussed in the preceding sections proceed at a finite rate and to a finite extent.

To what extent a reaction progresses is determined by its equilibrium state. Its kinetic rates, on the other hand, determine how fast the reaction products are formed and whether the reaction completes within the gasifier chamber. A review of the basics of chemical equilibrium may be useful before discussing its results.

5.4.1 Chemical Equilibrium

Let us consider the reaction:

$$nA + mB \xrightarrow{k_{for}} pC + qD \tag{5.27}$$

where *n, m, p,* and *q* are stoichiometric coefficients. The rate of this reaction, r_1, depends on C_A and C_B, the concentration of the reactants *A* and *B*, respectively.

$$r_1 = k_{for}\, C_A^n\, C_B^m \tag{5.28}$$

The reaction can also move in the opposite direction:

$$pC + qD \xrightarrow{k_{back}} nA + mB \tag{5.29}$$

The rate of this reaction, r_2, is similarly written in terms of C_C and C_D, the concentration of *C* and *D*, respectively:

$$r_2 = k_{back}\, C_C^p\, C_D^q \tag{5.30}$$

When the reaction begins, the concentration of the reactants *A* and *B* is high. So the forward reaction rate r_1 is initially much higher than r_2, the reverse reaction rate, because the product concentrations are relatively low. The reaction in this state is not in equilibrium, as $r_1 > r_2$. As the reaction progresses, the forward reaction increases the buildup of products *C* and *D*. This increases the reverse reaction rate. Finally, a stage comes when the two rates are equal to each other ($r_1 = r_2$). This is the equilibrium state. At equilibrium,

- There is no further change in the concentration of the reactants and the products.

- The forward reaction rate is equal to the reverse reaction rate.
- The Gibbs free energy of the system is at minimum.
- The entropy of the system is at maximum.

Under equilibrium state, we have

$$r_1 = r_2$$

$$k_{for}\, C_A^n\, C_B^m = k_{back}\, C_C^p\, C_D^q \tag{5.31}$$

Reaction Rate Constant

A rate constant, k_i, is independent of the concentration of reactants but is dependent on the reaction temperature, T. The temperature dependency of the reaction rate constant is expressed in Arrhenius form as

$$k = A_0 \exp\left(-\frac{E}{RT}\right) \tag{5.32}$$

where A_0 is a pre-exponential constant, R is the universal gas constant, and E is the activation energy for the reaction.

The ratio of rate constants for the forward and reverse reactions is the equilibrium constant, K_e. From Eq. (5.31) we can write

$$K_e = \frac{k_{for}}{k_{back}} = \frac{C_C^p C_D^q}{C_A^n C_B^q} \tag{5.33}$$

The equilibrium constant, K_e, depends on temperature but not on pressure. Table 5.4 gives values of equilibrium constants and heat of formation of some gasification reactions (Probstein and Hicks, 2006, pp. 62–64).

TABLE 5.4 Equilibrium Constants and Heats of Formation for Five Gasification Reactions

	Equilibrium Constant ($\log_{10}$K)			Heat of Formation (kJ/mol)	
Reaction	***298 K***	***1000 K***	***1500 K***	***1000 K***	***1500 K***
$C + \frac{1}{2} O_2 \rightarrow CO$	24.065	10.483	8.507	–111.9	–116.1
$C + O_2 \rightarrow CO_2$	69.134	20.677	13.801	–394.5	–395.0
$C + 2H_2 \rightarrow CH_4$	8.906	–0.999	–2.590	–89.5	–94.0
$2C + 2H_2 \rightarrow C_2H_4$	–11.940	–6.189	–5.551	38.7	33.2
$H_2 + \frac{1}{2} O_2 \rightarrow H_2O$	40.073	10.070	5.733	–247.8	–250.5

Source: Data compiled from Probstein and Hicks, 2006, p. 64.

Gibbs Free Energy

Gibbs free energy, G, is an important thermodynamic function. Its change in terms of a change in entropy, ΔS, and enthalpy, ΔH, is written as

$$\Delta G = \Delta H - T\Delta S \tag{5.34}$$

The change in enthalpy or entropy for a reaction system is computed by finding the enthalpy or entropy changes of individual gases in the system. It is explained in Example 5.2. An alternative approach uses the empirical equations given by Probstein and Hicks (2006). It expresses the Gibbs function (Eq. 5.35) and the enthalpy of formation (Eq. 5.36) in terms of temperature, T, the heat of formation at the reference state at 1 atmosphere and 298 K, and a number of empirical coefficients, a', b', and so forth.

$$\Delta G^0_{f,T} = \Delta h^0_{298} - a'T\ln(T) - b'T^2 - \left(\frac{c'}{2}\right)T^3 - \left(\frac{d'}{3}\right)T^4 + \left(\frac{e'}{2T}\right) + f' + g'T \quad \text{kJ/mol} \tag{5.35}$$

$$\Delta H^0_{f,T} = \Delta h^0_{298} + a'T + b'T^2 + c'T^3 + d'T^4 + \left(\frac{e'}{T}\right) + f' \quad \text{kJ/mol} \tag{5.36}$$

The values of the empirical coefficients for some common gases are given in Table 5.5.

The equilibrium constant of a reaction occurring at a temperature T may be known using the value of Gibbs free energy.

$$K_e = \exp\left(-\frac{\Delta G}{RT}\right) \tag{5.37}$$

Here, ΔG is the standard Gibbs function of reaction or free energy change for the reaction, R is the universal gas constant, and T is the gas temperature.

Example 5.2

Find the equilibrium constant at 2000 K for the reaction

$$CO_2 \rightarrow CO + \tfrac{1}{2}O_2$$

Solution

Enthalpy change is written by taking the values for it from the NIST-JANAF thermochemical tables (Chase, 1998) for 2000 K:

$$\begin{aligned}\Delta H &= (h_f^0 + \Delta h)_{CO} + (h_f^0 + \Delta h)_{O_2} - (h_f^0 + \Delta h)_{CO_2} \\ &= 1\,\text{mol}\,(-110,527 + 56,744)\,\text{J/mol} + 1/2\,\text{mol}\,(0 + 59,175)\,\text{J/mol} \\ &\quad - 1\,\text{mol}\,(-393,522 + 91,439)\,\text{J/mol} = 277,887\,\text{J}\end{aligned}$$

The change in entropy, ΔS, is written in the same way as for taking the values of entropy change from the NIST-JANAF tables (see list that follows on page 140).

TABLE 5.5 Heat of Combustion, Gibbs Free Energy, and Heat of Formation at 298 K, 1 Atm, and Empirical Coefficients from Eqs. 5.35 and 5.36

Product	*HHV* (kJ/mol)	$\Delta_f G_{298}$ (kJ/mol)	$\Delta_f H_{298}$ (kJ/mol)	Empirical Coefficients						
				a'	b'	c'	d'	e'	f'	g'
C	393.5	0	0							
CO	283	−137.3	−110.5	5.619×10^{-3}	-1.19×10^{-5}	6.383×10^{-9}	-1.846×10^{-12}	-4.891×10^{2}	0.868	-6.131×10^{-2}
CO_2	0	−394.4	−393.5	-1.949×10^{-2}	3.122×10^{-5}	-2.448×10^{-8}	6.946×10^{-12}	-4.891×10^{2}	5.27	−0.1207
CH_4	890.3	−50.8	−74.8	-4.62×10^{-2}	1.13×10^{-5}	1.319×10^{-8}	-6.647×10^{-12}	-4.891×10^{2}	14.11	0.2234
C_2H_4	1411	68.1	52.3	-7.281×10^{-2}	5.802×10^{-5}	-1.861×10^{-8}	5.648×10^{-13}	-9.782×10^{2}	20.32	−0.4076
CH_3OH	763.9	−161.6	−201.2	-5.834×10^{-2}	2.07×10^{-5}	1.491×10^{-8}	-9.614×10^{-12}	-4.891×10^{2}	16.88	−0.2467
H_2O (steam)	0	−228.6	−241.8	-8.95×10^{-3}	-3.672×10^{-6}	5.209×10^{-9}	-1.478×10^{-12}	0	2.868	−0.0172
H_2O (water)	0	−237.2	−285.8							
O_2	0	0	0							
H_2	285.8	0	0							

Source: Adapted from Probstein and Hicks, 2006, pp. 55, 61.

$$\begin{aligned}\Delta S &= 1\times S_{CO} + \tfrac{1}{2}\times S_{O_2} - 1\times S_{CO_2}\\ &= (1\,\text{mol}\times 258.71\,\text{J/mol K}) + (1/2\,\text{mol}\times 268.74\,\text{J/mol K})\\ &\quad - (1\,\text{mol}\times 309.29\,\text{J/mol K})\\ &= 83.79\,\text{J/K}\end{aligned}$$

From Eq. (5.34), the change in the Gibbs free energy can be written as

$$\begin{aligned}\Delta G &= \Delta H - T\Delta S\\ &= 277.887\,\text{kJ} - (2{,}000\,\text{K}\times 83.79\,\text{J/K}) = 110.307\,\text{kJ}\end{aligned}$$

The equilibrium constant is calculated using Eq. (5.37):

$$K_{2000K} = e^{-\frac{\Delta G}{RT}} = e^{-\left(\frac{110.307}{0.008314*2000}\right)} = 0.001315 \tag{5.38}$$

Kinetics of Gas–Solid Reactions

The rate of gasification of char is much slower than the rate of pyrolysis of the biomass that produces the char. Thus, the volume of a gasifier is more dependent on the rate of char gasification than on the rate of pyrolysis. The char gasification reaction therefore plays a major role in the design and performance of a gasifier.

Typical temperatures of the gasification zone in downdraft and fluidized-bed reactors are in the range of 700 to 900 °C. The three most common gas–solid reactions that occur in the char gasification zone are

$$\text{Boudouard reaction:}\quad (\text{R1: C} + \text{CO}_2 \rightarrow 2\text{CO}) \tag{5.39}$$

$$\text{Water}-\text{gas reaction:}\quad (\text{R2: C} + \text{H}_2\text{O} \leftrightarrow \text{CO} + \text{H}_2) \tag{5.40}$$

$$\text{Methanation reaction:}\quad (\text{R3: C} + 2\text{H}_2 \leftrightarrow \text{CH}_4). \tag{5.41}$$

The water–gas reaction, R2, is dominant in a steam gasifier. In the absence of steam, when air or oxygen is the gasifying medium, the Boudouard reaction, R1, is dominant. However, the steam gasification reaction rate is higher than the Boudouard reaction rate.

Another important gasification reaction is the shift reaction, R9 ($CO + H_2O \leftrightarrow CO_2 + H_2$), which takes place in the gas phase. It is discussed in the next section. A popular form of the gas–solid char reaction, r, is the nth-order expression:

$$r = \frac{1}{(1-X)^m}\frac{dX}{dt} = A_0 e^{-\frac{E}{RT}} P_i^n\ \text{s}^{-1} \tag{5.42}$$

where X is the fractional carbon conversion, A_0 is the apparent pre-exponential constant (1/s), E is the activation energy (kJ/mol), m is the reaction order with respect to the carbon conversion, T is the temperature (K), and n is the reaction

order with respect to the gas partial pressure, P_i. The universal gas constant, R, is 0.008314 kJ/mol.K.

Boudouard Reaction

Referring to the Boudouard reaction (R1) in Eq. (5.6), we can use the Langmuir–Hinshelwood rate, which takes into account CO inhibition (Cetin et al., 2005) to express the apparent gasification reaction rate, r_b:

$$r_b = \frac{k_{b1} P_{CO_2}}{1 + (k_{b2}/k_{b3}) P_{CO} + (k_{b1}/k_{b3}) P_{CO_2}} \ s^{-1} \tag{5.43}$$

where P_{CO} and P_{CO_2} are the partial pressure of CO and CO_2, respectively, on the char surface (bar). The rate constants, k_i, are given in the form, $A \exp(-E/RT)$ $bar^{-n}s^{-n}$, where A is the pre-exponential factor ($bar^{-n}.s^{-n}$). Barrio and Hustad (2001) gave some values of the pre-exponential factor and the activation energy for Birch wood (Table 5.6).

When the concentration of CO is relatively small, and when its inhibiting effect is not to be taken into account, the kinetic rate of gasification by the Boudouard reaction may be expressed by a simpler nth-order equation as

$$r_b = A_b e^{-\frac{E}{RT}} P_{CO_2}^n \ s^{-1} \tag{5.44}$$

For the Boudouard reaction, the values of the activation energy, E, for biomass char are typically in the range of 200 to 250 kJ/mol, and those of the exponent, n, are in the range of 0.4 to 0.6 (Blasi, 2009). Typical values of A, E, and n for birch, poplar, cotton, wheat straw, and spruce are given in Table 5.7.

The reverse of the Boudouard reaction has a major implication, especially in catalytic reactions, as it deposits carbon on its catalyst surfaces, thus deactivating the catalyst.

$$2CO \rightarrow CO_2 + C - 172 \ kJ/mol \tag{5.45}$$

TABLE 5.6 Activation Energy and Pre-Exponential Factors for Birch Char Using the Langmuir-Hinshelwood Rate Constants for CO_2 Gasification

Langmuir-Hinshelwood Rate Constants (s^{-1} bar^{-1})	Activation Energy, E (kJ/mol)	Pre-Exponential Actor, A (s^{-1} bar^{-1})
k_{b1}	165	1.3×10^5
k_{b2}	20.8	0.36
k_{b3}	236	3.23×10^7

Source: Adapted from Barrio and Hustad, 2001.

TABLE 5.7 Typical Values for Activation Energy, Pre-Exponential Factor, and Reaction Order for Char in the Boudouard Reaction

Char Origin	Activation Energy, E (kJ/mol)	Pre-Exponential Factor, A (s^{-1} bar^{-1})	Reaction Order, n (–)	Reference
Birch	215	3.1×10^6 s^{-1} $bar^{-0.38}$	0.38	Barrio and Hustad, 2001
Dry poplar	109.5	153.5 s^{-1} bar^{-1}	1.2	Barrio and Hustad, 2001
Cotton wood	196	4.85×10^8 s^{-1}	0.6	DeGroot and Shafizadeh, 1984
Douglas fir	221	19.67×10^8 s^{-1}	0.6	DeGroot and Shafizadeh, 1984
Wheat straw	205.6	5.81×10^6 s^{-1}	0.59	Risnes et al., 2001
Spruce	220	21.16×10^6 s^{-1}	0.36	Risnes et al., 2001

The preceding reaction becomes thermodynamically feasible when (P_{CO}^2/P_{CO_2}) is much greater than that of the equilibrium constant of the Boudouard reaction (Littlewood, 1977).

Water–Gas Reaction

Referring to the water–gas reaction, the kinetic rate, r_w, may also be written in Langmuir-Hinshelwood form to consider the inhibiting effect of hydrogen and other complexes (Blasi, 2009).

$$r_w = \frac{k_{w1} P_{H_2O}}{1 + (k_{w1}/k_{w3}) P_{H_2O} + (k_{w2}/k_{w3}) P_{H_2}} \text{ s}^{-1} \tag{5.46}$$

where P_i is the partial pressure of gas i in bars.

Typical rate constants according to Barrio et al. (2001) for beech wood are

$$k_{w1} = 2.0 \times 10^7 \exp(-199/RT); \text{ bar}^{-1}\text{s}^{-1}$$

$$k_{w2} = 1.8 \times 10^6 \exp(-146/RT); \text{ bar}^{-1}\text{s}^{-1}$$

$$k_{w3} = 8.4 \times 10^7 \exp(-225/RT) \text{ bar}^{-1}\text{s}^{-1}$$

Most kinetic analysis, however, uses a simpler nth-order expression for the reaction rate:

$$r_w = A_w e^{-\frac{E}{RT}} P_{H_2O}^n \text{ s}^{-1} \tag{5.47}$$

Typical values for the activation energy, E, for steam gasification of char for some biomass types are given in Table 5.8.

TABLE 5.8 Activation Energy, Pre-Exponential Factor, and Reaction Order for Char for the Water–Gas Reaction

Char Origin	Activation Energy, E (kJ/mol)	Pre-Exponential Factor, A_w (s^{-1} bar^{-1})	Reaction Order, n (–)	Reference
Birch	237	2.62×10^8 s^{-1} bar^{-n}	0.57	Barrio et al., 2001
Beech	211	0.171×10^8 s^{-1} bar^{-n}	0.51	Barrio et al., 2001
Wood	198	0.123×10^8 s^{-1} atm^{-n}	0.75	Hemati and Laguerie, 1988
Various biomass	180–200		0.04–1.0	Blasi, 2009

Hydrogasification Reaction (Methanation)

The hydrogasification reaction is as follows:

$$C + 2H_2 \Leftrightarrow CH_4 \tag{5.48}$$

With freshly devolatilized char, this reaction progresses rapidly, but graphitization of carbon soon causes the rate to drop to a low value. The reaction involves volume increase, and so pressure has a positive influence on it. High pressure and rapid heating help this reaction. Wang and Kinoshita (1993) measured the rate of this reaction and obtained values of $A = 4.189 \times 10^{-3}$ s^{-1} and $E = 19.21$ kJ/mol.

Steam Reforming of Hydrocarbon

For production of syngas (CO, H_2) direct reforming of hydrocarbon is an option. Here, a mixture of hydrocarbon and steam is passed over a nickel-based catalyst at 700 to 900 °C. The final composition of the product gas depends on the following factors (Littlewood, 1977):

- H/C ratio of the feed
- Steam/carbon (S/C) ratio
- Reaction temperature
- Operating pressure

The mixture of CO and H_2 produced can be subsequently synthesized into required liquid fuels or chemical feedstock. The reactions may be described as

$$C_nH_m + \frac{4m-n}{4}H_2O \Leftrightarrow \frac{4m+n}{8}CH_4 + \frac{4m-n}{8}CO_2 \tag{5.49}$$

$$CH_4 + H_2O \Leftrightarrow CO + 3H_2 \tag{5.50}$$

$$CO + H_2O \Leftrightarrow CO_2 + H_2 \tag{5.51}$$

The first reaction (Eq. 5.48) is favorable at high pressure, as it involves an increase in volume in the forward direction. The equilibrium constant of the first reaction increases with temperature while that of the third reaction (Eq. 5.51), which is also known as the shift reaction, decreases.

Kinetics of Gas-Phase Reactions

Several gas-phase reactions play an important role in gasification. Among them, the shift reaction (R9), which converts carbon monoxide into hydrogen, is most important.

$$\text{R9: } CO + H_2O \xrightarrow{k_{for}} CO_2 + H_2 - 41.1\ \text{kJ/mol} \tag{5.52}$$

This reaction is mildly exothermic. Since there is no volume change, it is relatively insensitive to changes in pressure.

The equilibrium yield of the shift reaction decreases slowly with temperature. For a favorable yield, the reaction should be conducted at low temperature, but then the reaction rate will be slow. For an optimum rate, we need catalysts. Below 400 °C, a chromium-promoted iron formulation catalyst ($Fe_2O_3 - Cr_2O_3$) may be used (Littlewood, 1977).

Other gas-phase reactions include CO combustion, which provides heat to the endothermic gasification reactions:

$$\text{R6: } CO + 1/2\,O_2 \xrightarrow{k_{for}} CO_2 - 284\ \text{kJ/mol} \tag{5.53}$$

These homogeneous reactions are reversible. The rate of forward reactions is given by the rate coefficients of Table 5.9.

TABLE 5.9 Forward Reaction Rates, r, for Gas-Phase Homogeneous Reactions

Reaction	Reaction Rate (r)	Heat of Formation ($m^3.mol^{-1}.s^{-1}$)	Reference
$H_2 + ½\,O_2 \rightarrow H_2O$	$K\,C_{H2}^{1.5}C_{O_2}$	$51.8\ T^{1.5}$ exp (–3420/T)	Vilienskii and Hezmalian, 1978
$CO + ½\,O_2 \rightarrow CO_2$	$K\,C_{CO}C_{O^2}^{0.5}C_{H2O}^{0.5}$	2.238×10^{12} exp (–167.47/RT)	Westbrook and Dryer, 1981
$CO + H_2O \rightarrow CO_2 + H_2$	$K\,C_{CO}C_{H_2O}$	0.2778 exp (–12.56/RT)	Petersen and Werther, 2005

Note: Here, the gas constant, R, is in kJ/mol.K.

For the backward CO oxidation reaction ($CO + \frac{1}{2} O_2 \xleftarrow{k_{back}} CO_2$), the rate, k_{back}, is given by Westbrook and Dryer (1981) as

$$k_{back} = 5.18 \times 10^8 \exp(-167.47/RT)\, C_{CO_2} \tag{5.54}$$

For the reverse of the shift reaction ($CO + H_2O \xleftarrow{k_{back}} CO_2 + H_2$), the rate is given as

$$k_{back} = 126.2 \exp(-47.29/RT) C_{CO_2} C_{H_2} \text{ mol.m}^{-3} \tag{5.55}$$

If the forward rate constant is known, then the backward reaction rate, k_{back}, can be determined using the equilibrium constant from the Gibbs free energy equation:

$$K_{equilibrium} = \frac{k_{for}}{k_{back}} = \exp\left(\frac{-\Delta G^0}{RT}\right) \text{at 1 atm pressure} \tag{5.56}$$

ΔG^0 for the shift reaction may be calculated (see Callaghan, 2006) from a simple correlation of

$$\Delta G^0 = -32.197 + 0.031T - (1774.7/T), \text{kJ/mol} \tag{5.57}$$

where T is in K.

Example 5.3

For shift reaction CO + $H_2O \rightarrow CO_2$ + H_2, the equilibrium constant at 625 K is given as 20 and that at 1667 K as 0.368. Assume that the reaction begins with 1 mole of CO, 1 mole of H_2O, and 1 mole of nitrogen. Find:

- The equilibrium constant at 1100 K and 1 atm.
- The equilibrium mole fraction of carbon dioxide.
- Whether the reaction is endothermic or exothermic.
- If pressure is increased to 100 atm, the impact of the equilibrium constant at 1100 K.

Solution

Part (a). For the shift reaction, the Gibbs free energy at a certain temperature can be calculated from Eq. (5.57):

$$\Delta G^0 = -32.197 + 0.031T - (1774.7/T)$$

at 1100 K, ΔG^0 = 0.2896 kJ/mol.

The equilibrium constant can be calculated from Eq. (5.56):

$$K_{equilibrium} = \frac{k_{for}}{k_{back}} = \exp\left(\frac{-\Delta G^0}{RT}\right)$$

$$K_{equilibrium} = \exp\left(\frac{-0.2896}{0.008314 * 1100}\right)$$

$$K_{equilibrium} = 0.9688$$

Part (b). At equilibrium, the rate of the forward reaction will be equal to the rate of the backward reaction, or $K_{equilibrium} = 1$. So, using the definition of the equilibrium constant, we have

$$K_{equilibrium} = \frac{p_{CO_2} p_{H_2}}{p_{CO} p_{H_2O}} = 1$$

where p denotes the partial pressure of the various species. In this reaction, nitrogen stays inert and does not react. Thus, 1 mole of nitrogen comes out from it. If x moles of CO and H_2O react to form x moles of CO_2 and H_2, then at equilibrium, $(1 - x)$ moles of CO and H_2O remain unreacted. We can list the component mole fraction as:

Species	Mole	Mole fraction
CO	$(1 - x)$	$(1 - x) / 3$
H_2O	$(1 - x)$	$(1 - x) / 3$
CO_2	x	$x/3$
H_2	x	$x/3$
N_2	1	1/3

The mole fraction y is related to the partial pressure, p, by the relation $yP = p$, where P stands for total pressure.

Substituting the values for the partial pressures of the various species,

$$1 = \frac{\left(\frac{x}{3}P\right)\left(\frac{x}{3}P\right)}{\left(\frac{1-x}{3}P\right)\left(\frac{1-x}{3}P\right)}$$

Solving for x, we get $x = 0.5$. Thus, the mole fraction of CO_2 at equilibrium = $(1 - x)/3 = 0.5/3 = 0.1667$.

Part (c). To determine if this reaction is exothermic or endothermic, the standard heats of formation of the individual components are taken from the NIST-JANAF thermochemical tables (Chase, 1998).

$$\Delta H = (h_f^0)_{CO_2} + (h_f^0)_{H_2} - \left[(h_f^0)_{CO} + (h_f^0)_{H_2O}\right]$$

$$\Delta H = -393.52\ \text{kJ/mol} - 0\ \text{kJ/mol} - [-110.53\ \text{kJ/mol} - 241.82\ \text{kJ/mol}]$$

$$\Delta H = -41.17\ \text{kJ/mol}$$

Since 41.17 kJ/mol of heat is given out, the reaction is exothermic.

Part (d). This reaction does not depend on pressure, as there is no volume change. The equilibrium constant changes only with temperature, so the equilibrium constant at 100 atm is the same as that at 1 atm, for 1100 K. The equilibrium constant is 0.9688 at 100 atm, for 1100 K.

5.4.2 Char Reactivity

Reactivity, generally a property of a solid fuel, is the value of the reaction rate under well-defined conditions of gasifying agent, temperature, and pressure.

Proper values or expressions of char reactivity are necessary for all gasifier models. This topic has been studied extensively for more than 60 years, and a large body of information is available, especially for coal. These studies unearthed important effects of char size, surface area, pore size distribution, catalytic effect, mineral content, pretreatment, and heating. The origin of the char and the extent of its conversion also exert some influence on reactivity.

Char can originate from any hydrocarbon—coal, peat, biomass, and so forth. An important difference between chars from biomass and those from fossil fuels like coal or peat is that the reactivity of biomass chars increases with conversion while that of coal or peat char decreases. Figure 5.3 plots the reactivity for hardwood and peat against their conversion (Liliedahl and Sjostrom, 1997). It is apparent that, while the conversion rate (at conversion 0.8) of hardwood char in steam is 9% per minute, that of peat char under similar conditions is only 1.5% per minute.

Effect of Pyrolysis Conditions

The pyrolysis condition under which the char is produced also affects the reactivity of the char. For example, van Heek and Muhlen (1990) noted that the reactivity of char (in air) is much lower when produced above 1000 °C compared to that when produced at 700 °C. High temperatures reduce the number of active sites of reaction and the number of edge atoms. Longer residence times at peak temperature during pyrolysis also reduce reactivity.

Effect of Mineral Matter in Biomass

Inorganic materials in fuels can act as catalysts in the char–oxygen reaction (Zolin et al., 2001). In coal, inorganic materials reside as minerals, whereas in biomass they generally remain as salts or are organically bound. Alkali metals, potassium, and sodium are active catalysts in reactions with oxygen-containing species. Dispersed alkali metals in biomass contribute to the high catalytic activity of inorganic materials in biomass. In coal, CaO is also dispersed, but at high temperatures it sinters and vaporizes, blocking micropores.

Inorganic matter also affects pyrolysis, giving char of varying morphological characteristics. Potassium and sodium catalyze the polymerization of volatile matter, increasing the char yield; at the same time they produce solid materials that deposit on the char pores, blocking them. During subsequent oxidation of the char, the alkali metal catalyzes this process. Polymerization of volatile matter dominates over the pore-blocking effect. A high pyrolysis temperature may result in thermal annealing or loss of active sites and thereby loss of char reactivity (Zolin et al., 2001).

Intrinsic Reaction Rate

Char gasification takes place on the surface of solid char particles, which is generally taken to be the outer surface area. However, char particles are highly

porous, and the surface areas of the inner pore walls are several orders of magnitude higher than the external surface area. For example, the actual surface area (BET) of an internal pore of a 1-mm-diameter beechwood char is 660 cm^2 while its outer surface is only 3.14 cm^2. Thus, if there is no physical restriction, the reacting gas can potentially enter the pores and react on their walls, resulting in a high overall char conversion rate. For this reason, two char particles with the same external surface area (size) may have widely different reaction rates because of their different internal structure.

From a scientific standpoint, it is wise to express the surface reaction rate on the basis of the actual surface on which the reaction takes place rather than the external surface area. The rate based on the actual pore wall surface area is the *intrinsic reaction rate*; the rate based on the external surface area of the char is the *apparent reaction rate*. The latter is difficult to measure, so sometimes it is taken as the reactive surface area determined indirectly from the reaction rate instead of the total pore surface area measured by the physical adsorption of nitrogen. This is known as the BET area (Klose and Wolki, 2005).

Mass Transfer Control

For the gasification reaction to take place within the char's pores, the reacting gas must enter the pores. If the availability of the gas is so limited that it is entirely consumed by the reaction on the outer surface of the char, gasification is restricted to the external surface area. This can happen because of the limitation of the mass transfer of gas to the char surface. We can illustrate using the example of char gasification in CO_2:

$$C + CO_2 \rightarrow 2CO \tag{5.58}$$

Here, the CO_2 gas has to diffuse to the char surface to react with the active carbon sites. The diffusion, however, takes place at a finite rate. If the kinetic rate of this reaction is much faster than the diffusion rate of CO_2 to the char surface, all of the CO_2 gas molecules transported are consumed on the external surface of the char, leaving none to enter the pores and react on their surfaces. As the overall reaction is controlled by diffusion, it is called the *diffusion-* or *mass-transfer-controlled* regime of reaction.

On the other hand, if the kinetic rate of reaction is slow compared to the transport rate of CO_2 molecules, then the CO_2 will diffuse into the pores and react on their walls. The reaction in this situation is "kinetically controlled."

$$\begin{aligned} &\text{Diffusion rate} >> \text{kinetic rate} \quad [\text{Kinetic control reaction}] \\ &\text{Diffusion rate} << \text{kinetic rate} \quad [\text{Diffusion control reaction}] \end{aligned} \tag{5.59}$$

Between the two extremes lie intermediate regimes. The relative rates of chemical reaction and diffusion determine the gas concentration profile in the vicinity of the char particle; how the reaction progresses; and how char size, pore distribution, reaction temperature, char gas relative velocity, and so forth,

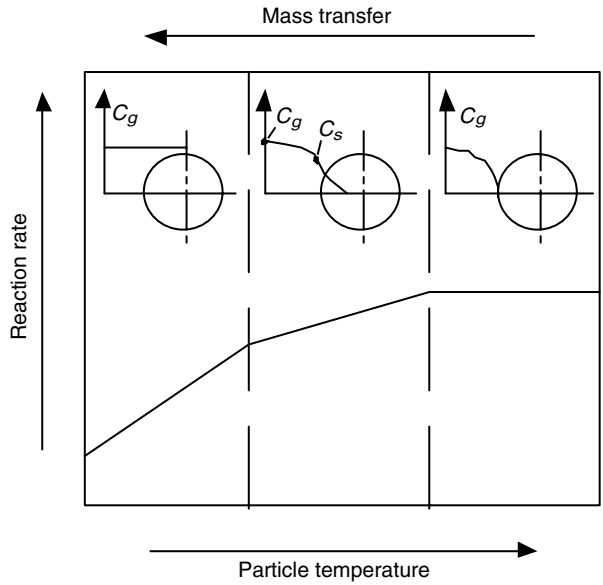

FIGURE 5.9 Char gasification regimes in a porous biomass char particle.

influence overall char conversion. Figure 5.9 shows how the concentration profile of CO_2 around the particle changes with temperature. With a rise in the surface temperature, the kinetic rate increases and therefore the overall reaction moves from the kinetic to the diffusion-controlled regime, resulting in less reaction within the pores.

The overall gasification rate of char particles, Q, when both mass transfer and kinetic rates are important, may be written as

$$Q = \frac{P_g}{\frac{1}{h_m} + \frac{1}{R_c}} \text{ kg Carbon}/\text{m}^2.\text{s} \tag{5.60}$$

where P_g is the concentration in partial pressure (bar) of the gasifying agent outside the char particle, h_m is the mass transfer rate (kg carbon/(m^2bar.s)) to the surface, and R_c is the kinetic rate of reaction: kg carbon/(m^2bar.s).

5.5 GASIFICATION MODELS

Optimal conversion of chemical energy of the biomass or other solid fuel into the desired gas depends on proper configuration, sizing, and choice of gasifier operating conditions. In commercial plants, optimum operating conditions are often derived through trials on the unit or by experiments on pilot plants. Even though expensive, experiments can give more reliable design data than can be obtained through modeling or simulation. There is, however, one major

limitation with experimental data. If one of the variables of the original process changes, the optimum operating condition chosen from the specific experimental condition is no longer valid. Furthermore, an experimentally found optimum parameter can be size-specific; that is, the optimum operating condition for one size of gasifier is not necessarily valid for any other size. The right choice between experiment and modeling, then, is necessary for a reliable design.

5.5.1 Simulation versus Experiment

Simulation, or mathematical modeling, of a gasifier may not give a very accurate prediction of its performance, but it can at least provide qualitative guidance on the effect of design and operating or feedstock parameters. Simulation allows the designer or plant engineer to reasonably optimize the operation or the design of the plant using available experimental data for a pilot plant or the current plant.

Simulation can also identify operating limits and hazardous or undesirable operating zones, if they exist. Modern gasifiers, for example, often operate at a high temperature and pressure and are therefore exposed to extreme operating conditions. To push the operation to further extreme conditions to improve the gasifier performance may be hazardous, especially if it is done with no prior idea of how the gasifier might behave at those conditions. Modeling may provide a less expensive means of assessing the benefits and the associated risk.

Simulation can never be a substitute for good experimental data, especially in the case of gas–solid systems such as gasifiers. A mathematical model, however sophisticated, is useless unless it can reproduce real operation with an acceptable degree of deviation (Souza-Santos, 2004). Still, a good mathematical model can

- Find optimum operating conditions or a design for the gasifier.
- Identify areas of concern or danger in operation.
- Provide information on extreme operating conditions (high temperature, high pressure) where experiments are difficult to perform.
- Provide information over a much wider range of conditions than one can obtain experimentally.
- Better interpret experimental results and analyze abnormal behavior of a gasifier, if that occurs.
- Assist scale-up of the gasifier from one successfully operating size to another, and from one feedstock to another.

5.5.2 Gasifier Simulation Models

Gasifier simulation models may be classified into the following groups:

- Thermodynamic equilibrium
- Kinetic

- Computational fluid dynamics (CFD)
- Artificial neural network

The thermodynamic equilibrium model predicts the maximum achievable yield of a desired product from a reacting system (Li et al., 2001). In other words, if the reactants are left to react for an infinite time, they will reach equilibrium yield. The yield and composition of the product at this condition is given by the equilibrium model, which concerns the reaction alone without taking into account the geometry of the gasifier.

In practice, only a finite time is available for the reactant to react in the gasifier. So, the equilibrium model may give an ideal yield. For practical applications, we need to use the kinetic model to predict the product from a gasifier that provides a certain time for reaction. A kinetic model studies the progress of reactions in the reactor, giving the product compositions at different positions along the gasifier. It takes into account the reactor's geometry as well as its hydrodynamics.

CFD models (Euler type) solve a set of simultaneous equations for conservation of mass, momentum, energy, and species over a discrete region of the gasifier. Thus, they give distribution of temperature, concentration, and other parameters within the reactor. If the reactor hydrodynamics is well known, a CFD model provides a very accurate prediction of temperature and gas yield around the reactor.

Neural network analysis is a relatively new simulation tool for modeling a gasifier. It works somewhat like an experienced operator, who uses his or her years of experience to predict how the gasifier will behave under a certain condition. This approach requires little prior knowledge about the process. Instead, the neural network *learns* by itself from sample experimental data (Guo et al., 1997).

Thermodynamic Equilibrium Models

Thermodynamic equilibrium calculation is independent of gasifier design and so is convenient for studying the influence of fuel and process parameters. Though chemical or thermodynamic equilibrium may not be reached within the gasifier, this model provides the designer with a reasonable prediction of the maximum achievable yield of a desired product. However, it cannot predict the influence of hydrodynamic or geometric parameters, like fluidizing velocity, or design variables, like gasifier height.

Chemical equilibrium is determined by either of the following:

- The equilibrium constant
- Minimization of the Gibbs free energy

Prior to 1958 all equilibrium computations were carried out using the equilibrium constant formulation of the governing equations (Zeleznik and Gordon,

1968). Later, computation of equilibrium compositions by Gibbs free energy minimization became an accepted alternative.

This section presents a simplified approach to equilibrium modeling of a gasifier based on the following overall gasification reactions:

$$\text{R1: } CO_2 + C \rightarrow 2\,CO \tag{5.61}$$

$$\text{R2: } C + H_2O \rightarrow H_2 + CO \tag{5.62}$$

$$\text{R3: } C + 2H_2 \rightarrow CH_4 \tag{5.63}$$

$$\text{R9: } CO + H_2O \rightarrow CO_2 + H_2 \tag{5.64}$$

From a thermodynamic point of view, the equilibrium state gives the maximum conversion for a given reaction condition. The reaction is considered to be zero dimensional and there are no changes with time (Li et al., 2001). An equilibrium model is effective at higher temperatures (>1500 K), where it can show useful trends in operating parameter variations (Altafini et al., 2003). For equilibrium modeling, one may use stoichiometric or nonstoichiometric methods (Basu, 2006).

Stoichiometric Equilibrium Models

In the stoichiometric method, the model incorporates the chemical reactions and species involved. It usually starts by selecting all species containing C, H, and O, or any other dominant elements. If other elements form a minor part of the product gas, they are often neglected.

Let us take the example of 1 mole of biomass being gasified in d moles of steam and e moles of air. The reaction of the biomass with air (3.76 moles of nitrogen, 1 mole of oxygen) and steam may then be represented by

$$\begin{aligned} CH_aO_bN_c + dH_2O + e(O_2 + 3.76N_2) \rightarrow\ & n_1C + n_2H_2 + n_3CO \\ & + n_4H_2O + n_5CO_2 + n_6CH_4 + n_7N_2 \end{aligned} \tag{5.65}$$

where $n_1 \ldots n_7$ are stoichiometric coefficients. Here, $CH_aO_bN_c$ is the chemical representation of the biomass and a, b, and c are the mole ratios (H/C, O/C, and N/C) determined from the ultimate analysis of the biomass. With d and e as input parameters, the total number of unknowns is seven.

An atomic balance of carbon, hydrogen, oxygen, and nitrogen gives

$$\text{C:}\quad n_1 + n_3 + n_5 + n_6 = 1 \tag{5.66}$$

$$\text{H:}\quad 2n_2 + 2n_4 + 4n_6 = a + 2d \tag{5.67}$$

$$\text{O:}\quad n_3 + n_4 + 2n_5 = b + d + 2e \tag{5.68}$$

$$\text{N:}\quad n_7 = c + 7.52e \tag{5.69}$$

During the gasification process, reactions R1, R2, R3, and R9 (see Table 5.2) take place. The water–gas shift reaction, R9, can be considered a result of the

subtraction of the steam gasification and Boudouard reactions, so we consider the equilibrium of reactions R1, R2, and R3 alone. For a gasifier pressure, P, the equilibrium constants for reactions R_1, R_2, and R_3 are given by

$$K_{e1} = \frac{y_{CO}^2 P}{y_{CO_2}} \quad \text{R1} \tag{5.70}$$

$$K_{e2} = \frac{y_{CO} y_{H_2} P}{y_{H_2O}} \quad \text{R2} \tag{5.71}$$

$$K_{e3} = \frac{y_{CH_4}}{y_{H_2}^2 P} \quad \text{R3} \tag{5.72}$$

where y_i is the mole fraction for species i of CO, H_2, H_2O, and CO_2.

The two sets of equations (stoichiometric and equilibrium) may be solved simultaneously to find the coefficients, $(n_1 \ldots n_7)$, and hence the product gas composition in an equilibrium state. Thus, by solving seven equations (Eqs. 5.66–5.72) we can find seven unknowns $(n_1 \ldots n_7)$, which give both the yield and the product of the gasification for a given air/steam-to-biomass ratio. The approach is based on the simplified reaction path and the chemical formula of the biomass.

This is a greatly simplified example of the stoichiometric modeling of a gasification reaction. The complexity increases with the number of equations considered. For a known reaction mechanism, the stoichiometric equilibrium model predicts the maximum achievable yield of a desired product or the possible limiting behavior of a reacting system.

Nonstoichiometric Equilibrium Models

In nonstoichiometric modeling, no knowledge of a particular reaction mechanism is required to solve the problem. In a reacting system, a stable equilibrium condition is reached when the Gibbs free energy of the system is at the minimum. So, this method is based on minimizing the total Gibbs free energy. The only input needed is the elemental composition of the feed, which is known from its ultimate analysis. This method is particularly suitable for fuels like biomass, the exact chemical formula of which is not clearly known.

The Gibbs free energy, G_{total} for the gasification product comprising N species $(i = 1 \ldots N)$ is given by

$$G_{total} = \sum_{i=1}^{N} n_i \Delta G_{f,i}^0 + \sum_{i=1}^{N} n_i RT \ln\left(\frac{n_i}{\sum n_i}\right) \tag{5.73}$$

where $\Delta G_{f,i}^0$ is the Gibbs free energy of formation of species i at standard pressure of 1 bar.

Equation (5.73) is to be solved for unknown values of n_i to minimize G_{total}, bearing in mind that it is subject to the overall mass balance of individual

elements. For example, irrespective of the reaction path, type, or chemical formula of the fuel, the amount of carbon determined by ultimate analysis must be equal to the sum total of all carbon in the gas mixture produced. Thus, for each *j*th element we can write

$$\sum_{i=1}^{N} a_{i,j} n_i = A_j \tag{5.74}$$

where $a_{i,j}$ is the number of atoms of the *j*th element in the *i*th species, and A_j is the total number of atoms of element *j* entering the reactor. The value of n_i should be found such that G_{total} will be minimum. We can use the Lagrange multiplier methods to solve these equations.

The Lagrange function (L) is defined as

$$L = G_{total} - \sum_{j=1}^{K} \lambda_j \left(\sum_{i=1}^{N} a_{ij} n_i - A_j \right) \text{kJ/mol} \tag{5.75}$$

where λ is the Lagrangian multiplier for the *j*th element.

To find the extreme point, we divide Eq. (5.75) by RT and take the derivative,

$$\left(\frac{\partial L}{\partial n_i} \right) = 0 \tag{5.76}$$

Substituting the value of G_{total} from Eq. (5.73) in Eq. (5.75), and then taking its partial derivative, the final equation is of the form given by

$$\left(\frac{\partial L}{\partial n_i} \right) = \frac{\Delta G^0_{f,i}}{RT} + \sum_{i=1}^{N} \ln \left(\frac{n_i}{n_{total}} \right) + \frac{1}{RT} \sum_{j=1}^{K} \lambda_j \left(\sum_{i=1}^{N} a_{ij} n_i \right) = 0 \tag{5.77}$$

Kinetic Models

Gas composition measurements for gasifiers often vary significantly from those predicted by equilibrium models (Peterson and Werther, 2005; Li et al., 2001; Kersten, 2002). This shows the inadequacy of equilibrium models and underscores the need of kinetic models to simulate gasifier behavior.

A kinetic model gives the gas yield and product composition a gasifier achieves after a finite time (or in a finite volume in a flowing medium). Thus, it involves parameters such as reaction rate, residence time of particles, and reactor hydrodynamics. For a given operating condition and gasifier configuration, the kinetic model can predict the profiles of gas composition and temperature inside the gasifier and overall gasifier performance.

The model couples the hydrodynamics of the gasifier reactor with the kinetics of gasification reactions inside the gasifier. At low reaction temperatures, the reaction rate is very slow, so the residence time required for complete conversion is long. Therefore, kinetic modeling is more suitable and accurate

at relatively low operating temperatures (<800 °C) (Altafini et al., 2003). For higher temperatures, where the reaction rate is faster, the equilibrium model may be of greater use.

Kinetic modeling has two components: (1) reaction kinetics and (2) reactor hydrodynamics.

Reaction Kinetics

Reaction kinetics must be solved simultaneously with bed hydrodynamics and mass and energy balances to obtain the yields of gas, tar, and char at a given operating condition.

As the gasification of a biomass particle proceeds, the resulting mass loss is manifested either through reduction in size with unchanged density or reduction in density with unchanged size. In both cases the rate is expressed in terms of the external surface area of the biomass char. Some models, where the reaction is made up of char alone, can define a reaction rate based on reactor volume. There are thus three ways of defining the char gasification reaction for biomass: (1) shrinking core model, (2) shrinking particle model, and (3) volumetric reaction rate model.

Reactor Hydrodynamics

The kinetic model considers the physical mixing process and therefore requires knowledge of reactor hydrodynamics. The hydrodynamics may be defined in terms of the following types with increasing sophistication and accuracy:

- Zero dimensional (stirred tank reactor)
- One dimensional (plug flow)
- Two dimensional
- Three dimensional

Unlike other models, the kinetic model is sensitive to the gas–solid contacting process involved in the gasifier. Based on this process, the model may be divided into three groups: (1) moving or fixed bed, (2) fluidized bed, and (3) entrained flow. Short descriptions of these are given in Section 5.6.

Neural Network Models

An alternative to the sophisticated modeling of a complex process, especially for one not well understood, is an artificial neural network (ANN). An ANN model mimics the working of the human brain and provides some human characteristics in solving models (Abdulsalam, 2005). It cannot produce an analytical solution, but it can give numerical results. This technique has been used with reasonable success to predict gas yield and composition from gasification of bagasse, cotton stem, pine sawdust, and poplar in fluidized beds (Guo et al., 1997); in municipal solid waste; and also in a fluidized bed (Xiao et al., 2009).

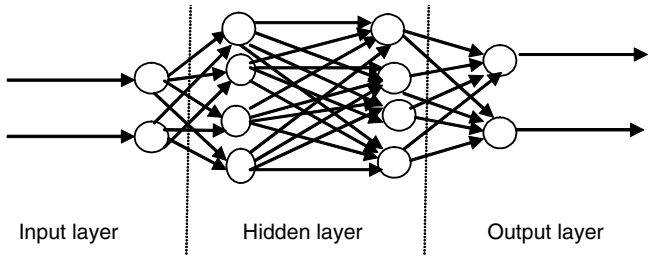

FIGURE 5.10 Schematic of a multilayer feed-forward neural network. *(Source: Adapted from Kalogirou, 2001.)*

The ANN model can deal with complex gasification problems. It uses a high-speed architecture of three hidden layers of neurons (Kalogirou, 2001): one to receive the input(s), one to process them, and one to deliver output(s). Figure 5.10 shows the arrangement of neuron layers and the connection patterns between them. Kalogirou (2001) suggested the following empirical formula to estimate the number of hidden neurons:

$$\text{Number of hidden neurons} = \tfrac{1}{2}(\text{inputs} + \text{outputs}) + \sqrt{\text{number of training patterns}} \tag{5.78}$$

The input layer has two values associated with it: inputs and weights. Weights are used to transfer data from layer to layer. In the first step, the information is processed at the nodes and then added up (summation); the result is passed through an activation function. The outcome is the node's "activation value," which is multiplied by the specific weight and transferred to the next node.

Network Training

Training modifies the connection weights in some orderly fashion using learning methods (Guo et al., 2001). It begins with a set of data (with inputs and outputs targeted); the weights are adjusted until the difference between the neural network output and the corresponding target is minimum (Kalogirou et al., 1999). When the training process satisfies the required tolerance, the network holds the weights constant and uses the network to make output predictions. After training, the weights contain meaningful information. A back-propagation algorithm is used to train the network. Multilayer feed-forward neural networks are used to approximate the function.

A neural network may return poor results for data that differ from the original data it was trained with. This happens sometimes when limited data are available to calibrate and evaluate the constants of the model (Hajek and Judd, 1995). After structuring the neural network, information starts to

flow from the input layer to the output layer according to the concepts described here.

CFD Models

Computational fluid dynamics can have an important role in the modeling of a fluidized-bed gasifier. A CFD-based code involves a solution of conservation of mass, momentum, species, and energy over a defined domain or region. The equations can be written for an element, where the flux of the just-mentioned quantities moving in and out of the element is considered with suitable boundary conditions.

A CFD code for gasification typically includes a set of submodels for the sequence of operations such as the vaporization of a biomass particle, its pyrolysis (devolatilization), the secondary reaction in pyrolysis, and char oxidation (Di Blasi, 2008; Babu and Chaurasia, 2004). Further sophistications such as a subroutine for fragmentation of fuels during gasification and combustion are also developed (Syred et al., 2007). These subroutines can be coupled with the transport phenomenon, especially in the case of a fluidized-bed gasifier.

The hydrodynamic or transport phenomenon for a laminar flow situation is completely defined by the Navier-Stokes equation, but in the case of turbulent flow a solution becomes difficult. A complete time-dependent solution of the instantaneous Navier-Stokes equation is beyond today's computation capabilities (Wang and Yan, 2008), so it is necessary to assume some models for the turbulence. The Reynolds-averaged Navier-Stokes (k-ε) model or large eddy simulation filters are two means of accounting for turbulence in the flow.

For a fluidized bed, the flow is often modeled using the Eulerian-Lagrange concept. The discrete phase is applied to the particle flow; the continuous phase, to the gas. Overmann and associates (2008) used the Euler-Euler and Euler-Lagrange approaches to model wood gasification in a bubbling fluidized bed. Their preliminary results found both to have comparable agreement with experiments. If the flow is sufficiently dilute, the particle–particle interaction and the particle volume in the gas are neglected.

A two-fluid model is another computational fluid dynamics approach. Finite difference, finite element, and finite volume are three methods used for discretization. Commercial software such as ANSYS, ASPEN, Fluent, Phoenics, and CFD2000 are available for solution (Miao et al., 2008). A review and comparison of these codes is given in Xia and Sun (2002) and Norton et al. (2007).

Recent progress in numerical solution and modeling of complex gas–solid interactions has brought CFD much closer to real-life simulation. If successful, it will be a powerful tool for optimization and even design of thermochemical reactors like gasifiers (Wang and Yan, 2008). CFD models are most effective in modeling entrained-flow gasifiers, where the gas–solid flows are less complex than those in fluidized beds and the solid concentration is low.

Models developed by several investigators employ sophisticated reaction kinetics and complex particle–particle interaction. Most of them, however, must use some submodels, fitting parameters or major assumptions into areas where precise information is not available. Such weak links in the long array make the final result susceptible to the accuracy of those "weak links." If the final results are known, we can use them to back-calculate the values of the unknown parameters or to refine the assumptions used.

The CFD model can thus predict the behavior of a given gasifier over a wider range of parameters using data for one situation, but this prediction might not be accurate if the code is used for a different gasifier with input parameters that are substantially different from the one for which experimental data are available.

5.6 KINETIC MODEL APPLICATIONS

This section briefly discusses how kinetic models can be applied to the three major gasifier types.

5.6.1 Moving-Bed Gasifiers

A basic moving-bed or fixed-bed gasifier can use the following assumptions:

- The reactor is uniform radially (i.e., no temperature or concentration gradient exists in the radial direction).
- The solids flow downward (in a updraft gasifier) as a plug flow.
- The gas flows upward as a plug flow.
- The interchange between two phases takes place by diffusion.

The mass balance of a gas species, j, can be written (Souza-Santos, 2004, p. 134) as

$$u_g \frac{d\rho_{g,j}}{dz} = D_{g,j} \frac{d^2\rho_{g,j}}{dz^2} + R_{m,j} \tag{5.79}$$

where u_g is the superficial gas velocity, z is the distance, $\rho_{g,j}$ is the density of the jth gas, and $D_{g,j}$ is the diffusivity of the jth gas. $R_{m,j}$, the production or consumption of the jth gas element, is related to $Q_{gasification}$ heat generation or absorption.

Similarly, an energy balance equation can be written for a dz element as

$$\rho_g C_{pg} u_g \frac{dT}{dz} = \lambda_g \frac{d^2T}{dz^2} + Q_{gasification} + Q_{conv} + Q_{rad} + Q_{mass} \tag{5.80}$$

where, $Q_{gasification}$, Q_{conv}, Q_{rad}, and Q_{mass} are the net heat flow into the element due to gasification, convection, radiation, and mass transfer, respectively. These terms can be positive or negative. ρ_g, C_{pg}, and λ_g are the density, specific heat, and thermal conductivity of the bulk gas, respectively.

Equations (5.79) and (5.80) can be solved simultaneously with appropriate expression for the reaction rate, $R_{m,j}$.

5.6.2 Fluidized-Bed Gasifiers

The kinetic modeling of fluidized-bed gasifiers requires several assumptions or submodels. It takes into account how the fluidized-bed hydrodynamics is viewed in terms of heat and mass transfer, and gas flow through the fluidized bed. The bed hydrodynamics defines the transport of the gasification medium through the system, which in turn influences the chemical reaction on the biomass surface. Each of these is subject to some assumptions or involves submodels.

One can use several versions of the fluidization model:

- Two-phase model of bubbling fluidized bed: bubbling and emulsion phases
- Three-phase model of bubbling fluidized bed: bubbling, cloud, and emulsion phases
- Fluidized bed divided into horizontal sections or slices
- Core-annulus structure

Gas flow through the bed can be modeled as:

- Plug flow in the bubbling phase; ideally mixed gas in the emulsion phase
- Ideally mixed gases in both phases
- Plug flow in both phases (there is exchange between phases)
- Plug flow through the bubble and emulsion phases without mass transfer between phases
- Plug flow of gas upward in the core and solid backflow in the annulus

The following sections present the essentials of a model for a circulating fluidized-bed combustor and one for a bubbling fluidized-bed gasifier (Kaushal et al., 2008). A typical one-dimensional steady-state model of a circulating fluidized-bed combustor, as shown in Figure 5.11, assumes gases as ideal and in the plug-flow regime. The riser is divided into three hydrodynamic zones: lower dense bed zone, intermediate middle zone, and top dilute zone. The solids are assumed uniform in size with no attrition. Char is a homogeneous matrix of carbon, hydrogen, and oxygen.

A bubbling fluidized-bed gasifier is divided into several zones with different hydrodynamic characteristics: dense zone and freeboard zone for bubbling beds; core-annulus for circulating beds. The dense zone additionally deals with the drying and devolatilization of the introduced feed. Superheated steam is introduced at the lower boundary of the dense zone. Each zone is further divided into cells, which individually calculate their local hydrodynamic and thermodynamic state using chosen equations or correlations. The cells are solved sequentially from bottom to top, with the output of each considered the input for the next. The conservation equations for carbon, bed material, and energy are evaluated not in each cell but across the entire zone. Therefore, each

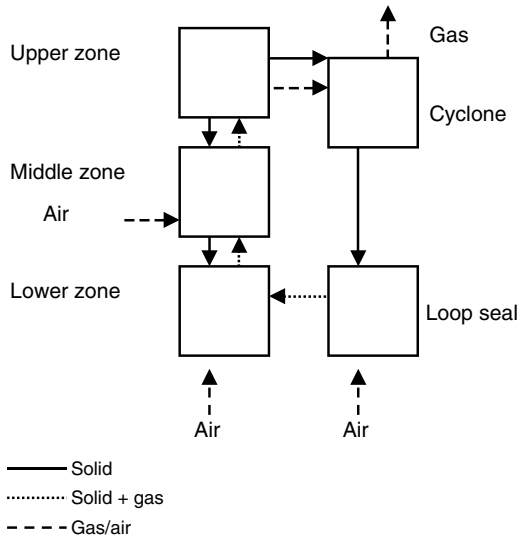

FIGURE 5.11 Model of a circulating fluidized-bed gasifier.

zone shows a homogeneous char concentration in the bed material and a uniform temperature. Additional input parameters to the model are geometric data, particle properties, and flow rates.

Hydrodynamic Submodel (Bubbling Bed)

The dense zone (assumed to be the bubbling bed) is modeled according to the modified two-phase theory. Bubble size is calculated as a function of bed height (Darton and LaNauze, 1977), and it is assumed that all bubbles at any cross-section are of uniform size:

$$d_b = 0.54\frac{(U-U_{mf})^{0.4}}{g^{0.2}}\left(z+4\sqrt{\frac{A}{N_{or}}}\right)^{0.8} \tag{5.81}$$

where A/N_{or} is the number of orifices per unit of cross-section area of the bed.

The interphase mass transfer between bubbles and emulsion, essential for the gas–solid reactions, is modeled semi-empirically using the specific bubble surface as the exchange area, the concentration gradient, and the mass-transfer coefficient. The mass-transfer coefficient, K_{BE}, based on the bubble–emulsion surface area (Sit and Grace, 1978), is

$$K_{BE} = \frac{U_{mf}}{4} + \sqrt{\frac{4\varepsilon_{mf} D_r U_B}{\pi d_B}} \tag{5.82}$$

where U_{mf} and ε_{mf} are, respectively, fluidization velocity and voidage at a minimum fluidizing condition, D_r is the bed diameter, and U_B is the rise velocity of a bubble of size d_B.

The axial mean voidage in the freeboard is calculated using an exponential decay function.

Reaction Submodel

Gasification reactions proceed at a finite speed; this process is divided into three steps: drying, devolatilization, and gasification. The time taken for drying and devolatilization of the fuel is much shorter than the time taken for gasification of the remaining char. Some models assume instantaneous drying and devolatilization because the rate of reaction of the char, which is the slowest, largely governs the overall process.

The products of devolatilization are CO_2, CO, H_2O, H_2, and CH_4. The gases released during drying and devolatilization are not added instantaneously to the upflowing gas stream, but are added along the height of the gasifier in a predefined pattern. The total mass devolatilized, $m_{volatile}$, is therefore the sum of the carbon, hydrogen, and oxygen volatilized from the solid biomass.

$$m_{volatile} = m_{char} + m_{hydrogen} + m_{oxygen} \tag{5.83}$$

Char gasification, the next critical step, may be assumed to move simultaneously through reactions R1, R2, and R3 (Table 5.2). As these three reactions occur simultaneously on the char particle, reducing its mass, the overall rate is given as

$$m_{char} = m_{Boudouard} + m_{steam} + m_{methanation} \tag{5.84}$$

The conversion of the porous char particle may be modeled assuming that the process follows shrinking particle (diminishing size), shrinking core (diminishing size of the unreacted core), or progressive conversion (diminishing density). The shift reaction is the most important homogenous reaction followed by steam reforming. The bed materials may catalyze the homogeneous reactions, but only in the emulsion phase, because the bubble phase is assumed to be free of solids.

5.6.3 Entrained-Flow Gasifiers

Extensive work on the modeling of entrained-flow gasifiers is available in the literature. Computational fluid dynamics (CFD) has been successfully applied to this gasifier type. This section presents a simplified approach to entrained-flow gasification following the work of Vamvuka et al. (1995).

The reactor is considered to be a steady-state, one-dimensional plug–flow reactor in the axial direction and well mixed radially—similar to that shown in Figure 5.12. Fuel particles shrink as they are gasified. Five gas–solid reactions (R1–R5 in Table 5.2) can potentially take place on the char particle surface. The reduction in the mass of char particles is the sum of these individual reactions, so if there are N_c char particles in the unit gas volume, the total reduction, W_c, in the plug flow is as shown in the equation that follows the figure.

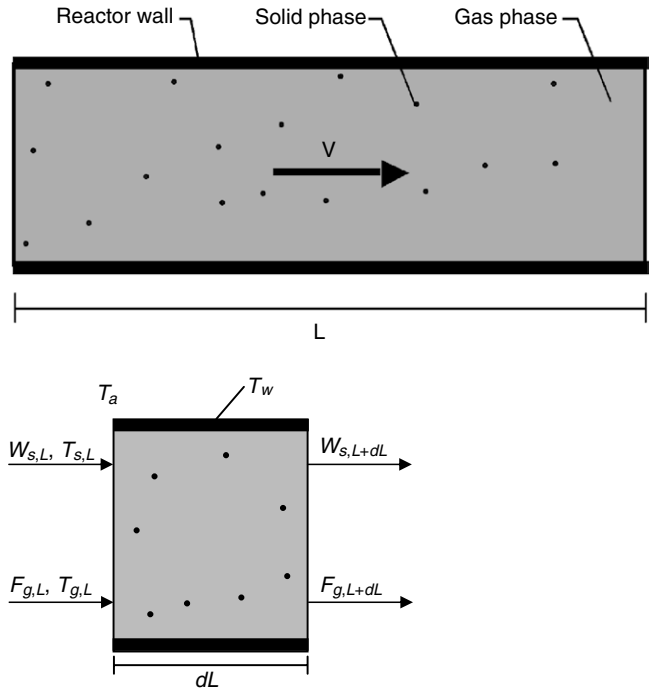

FIGURE 5.12 One-dimensional entrained-flow model.

$$dW_c = -(N_c A dz)\sum_{k=1}^{5} r_k(T_s, L_r) \tag{5.85}$$

where $r_k(T_s, L_r)$ is the surface reaction rate of the kth reaction (one of R1–R5) at the reactor's surface temperature, T_s, and length, L_r. A is its cross-section area.

Gaseous reactants diffuse to the char surface to participate in k reactions. Thus, if a_{jk} is the mass of the jth gas, required for the kth reaction, the overall diffusion rate of this gas from free stream concentration, y_j, to the char surface, y_{js}, may be related to the total of all reactions consuming the jth gas as follows:

$$\sum_{k=1}^{5} a_{jk} r_k(T_s, L_r) = 4\pi r_c^2 \left[\frac{D_{gj} P}{R T_g r_c}(y_j - y_{js})\right] \tag{5.86}$$

where y_{js} and y_j are mole fractions of gas on the char surface and in the bulk gas, respectively; P is the reactor pressure; and D_{gj} is the diffusion coefficient of the jth gas in the mixture of gases.

The surface reaction rate, $r_k(T_s,L_r)$, may be written in nth-order form as

$$r_k(T_s, L_r) = 4\pi r_c{}^2 K_{sk}(T_s)(P y_{js})^n \text{ mol/s} \tag{5.87}$$

where n is the order or reaction, and $K_{sk}(T_s)$ is the surface reaction rate constant at temperature T_s.

For conversion of gaseous species, we can write

$$\frac{dF_{gj}}{dZ} = \pm N_c A \sum_{k=1}^{5} a_{jk} r_k(T_s, L_r) \tag{5.88}$$

where $a_{j,k}$ is the stoichiometric coefficient for the jth gas in the kth reaction.

The total molar flow rate of the jth gas is found by adding the contribution of each of nine gas–solid and gas–gas reactions:

$$F_{gj} = F_{gj0} + \sum a_{jk} \xi_k \tag{5.89}$$

where F_{gj0} is the initial flow rate of the gas.

Energy Balance

Some of the five equations (reactions R1–R5) are endothermic while some are exothermic. The overall heat balance of reacting char particles is known from a balance of a particle's heat generation and heat loss to the gas by conduction and radiation.

$$\begin{aligned}\frac{d(W_c C_{pc} T_s)}{dZ} = &-N_c A \left[\sum_{k=1}^{5} r_k(T_s, L_r)\right] \Delta H_k(T_s) \\ &+ 4\pi r_c^2 \left[\frac{\lambda_g}{r_c}(T_s - T_g) + \sigma_p \sigma \left(T_c^4 - T_g^4\right)\right]\end{aligned} \tag{5.90}$$

where C_{pc} is the specific heat of the char, ΔH_k is the heat of reaction of the kth reaction at the char surface at temperature T_s, e_p is the emissivity of the char particle, λ_g is the thermal conductivity of the gas, and σ is the Stefan-Boltzmann constant.

A similar heat balance for the gas in an element dz in length can be carried out as

$$\begin{aligned}\frac{d\left(\sum_j F_{gj} C_{pg} T_g\right)}{dZ} = &-A\left[\sum_{k=6}^{9} \xi_k \Delta H_k(T_g)\right] \\ &- 4\pi r_c^2 N_C A \left[\frac{\lambda_g}{r_c}(T_g - T_c) + e_p \sigma \left(T_g^4 - T_c^4\right)\right] \\ &- \left[h_{conv}(T_g - T_w) + e_w \sigma \left(T_g^4 - T_w^4\right)\right] \pi D_r\end{aligned} \tag{5.91}$$

where $\Delta\xi_k$ is the extent of the gas-phase kth reaction with the heat of reaction, $\Delta H_k\ (T_g)$; h_{conv} is the gas-wall convective heat transfer coefficient; and D_r is the reactor's internal diameter.

The first term on the right of Eq. (5.91) is the net heat absorption by the gas-phase reaction, the second is the heat transfer from the gas to the char particles, and the third is the heat loss by the gas at temperature T_g to the wall at temperature T_w.

The equations are solved for an elemental volume, $A_r dL_r$, with boundary conditions from the previous upstream cell. The results are then used to solve the next downstream cell.

Symbols and Nomenclature

A = cross-sectional area of bed or reactor (m^2)
A_0 = pre-exponential coefficient in Eq. (5.42) (s^{-1})
A_b, A_w = pre-exponential coefficients in Eqs. (5.44) and (5.47), respectively (bar^{-n} s^{-1})
A_j = total number of atoms of element j entering the reactor (–)
$a_{i,j}$ = number of atoms of jth element in ith species (–)
a_{jk} = mass of jth gas, required for the kth reaction (kg)
C_i = molar concentration of ith gas (mol/m^3)
C_{pc} = specific heat of char (kJ/kg.K)
C_{pg} = specific heat of the bulk gas
D_r = internal diameter of the reactor (m)
$D_{g,j}$ = diffusion coefficient of the jth gas in the mixture of gases (m^2/s)
d_b = diameter of the bubble (m)
E = activation energy (kJ/mol)
e_p = emissivity of char particle (–)
F_{gl0} = initial flow rate of the gas (mol/s)
F_{gl} = molar flow rate of the lth gas (mol/s)
G_{total} = total Gibbs free energy (kJ)
g = acceleration due to gravity, 9.81 (m/s^2)
ΔH_k = heat of reaction of kth reaction at char surface (kJ/mol)
ΔH = enthalpy change (kJ)
h_i^0, h_f^0 = heat of formation at reference state (kJ)
h_{conv} = gas-wall convective heat transfer coefficient (kW/m^2K)
h_m = mass-transfer coefficient (kg carbon/m^2.bar^2.s)
k = first-order reaction rate constant (s^{-1})
k_0 = pre-exponential factor (s^{-1})
k_{liq} = rate constant for the liquid yield of pyrolysis (s^{-1})
k_{BE} = bubble-emulsion mass exchange coefficient (m/s)
k_c = rate constant for the char yield of pyrolysis (s^{-1})
k_g = rate constant for the gas yield of pyrolysis (s^{-1})
k_1 = rate constant of three primary pyrolysis reactions taken together (s^{-1})
K = number of element in Eq (5.77)
k_{w1}, k_{w2}, k_{w3} = rate constants in Eq (5.47) (bar^{-1} s^{-1})
K_{sk} = surface reaction rate constant for kth reaction, mol/m^2.bar^n
K_e, $K_{equilibrium}$ = equilibrium constant (–)
l = number of gaseous reactants (–)
L_r = length of the reactor (m)
L = Lagrangian function (–)
m_b = mass of the biomass in the primary pyrolysis process (kg)
m_0 = initial mass of the biomass (kg)
m_c = mass of the biomass remaining after complete conversion (kg)
m = reaction order with respect to carbon conversion in Eq. 5.42 (–)

m, n, p, q = stoichiometric coefficients in Eqs. 5.27–5.29
n = reaction order with respect to the gas partial pressure, Eq. 5.44 (–)
N = number of species present (–)
N_c = number of char particles in unit gas volume (–)
N_{or} = number of orifices in a bed of area (A_r)
P_i = partial pressure of the species i (bar)
P = total pressure of the species (bar)
Q = char gasification rate (kg carbon/m^2.s)
$Q_{gasification}$, Q_{conv}, Q_{rad}, and Q_{mass} = energy transfer due to gasification, convection, radiation, respectively (kW/m^3 of bed)
R = gas constant (8.314 J/mol.K, or 8.314×10^{-5} m^3.bar/mol.K)
R_c = chemical kinetic reaction rate (kg carbon/m^2.bar^{2}s)
$R_{m,g,j}$ = rate of production or consumption of gas species j (kg/m^{3}s)
r_i = reaction rate of the ith reaction (s^{-1})
r_c = char particle radius (m)
T = temperature (K)
T_s = surface temperature of char particles (K)
T_g = gas temperature (K)
T_w = wall temperature (K)
t = time (s)
u_g = superficial gas velocity in Eq. 5.80 (m/s)
U = fluidization velocity (m/s)
U_B = bubble rise velocity (m/s)
U_{mf} = minimum fluidization velocity (m/s)
X = fractional change in the carbon mass of the biomass (kg)
y = mole fraction of a species (–)
y_l = mole fraction of gas in the bulk (–)
y_{ls} = mole fraction of gas on the char surface (–)
z = height above grid or distance along a reactor from fuel entry (m)
α_{lk} = stoichiometric coefficient for lth gas in kth reaction (–)
β = partition coefficient (–)
λ = Lagrangian multiplier (–)
λ_g = thermal conductivity of gas (kJ/m.K)
σ = Stefan-Boltzmann constant (5.67×10^{-8} W m^{-2} K^{-4})
$\Delta G, \Delta G^0$ = change in Gibbs free energy (kJ)
ΔG_{fi}^0 = change in Gibbs free energy of formation of species i (kJ)
$\Delta \xi_k$ = extent of gas-phase kth reaction (–)
ρ_j = density of jth gas (kg/m^3)
ε_{mf} = voidage at minimum fluidization condition
ρ_g = density of the bulk gas
ΔS = entropy change (kJ/K)